

Simultaneous determination of CKM angle γ and charm mixing parameters



The LHCb collaboration

E-mail: matthew.william.kenzie@cern.ch

ABSTRACT: A combination of measurements sensitive to the CP violation angle γ of the Cabibbo-Kobayashi-Maskawa unitarity triangle and to the charm mixing parameters that describe oscillations between D^0 and \bar{D}^0 mesons is performed. Results from the charm and beauty sectors, based on data collected with the LHCb detector at CERN's Large Hadron Collider, are combined for the first time. This method provides an improvement on the precision of the charm mixing parameter y by a factor of two with respect to the current world average. The charm mixing parameters are determined to be $x = (0.400^{+0.052}_{-0.053})\%$ and $y = (0.630^{+0.033}_{-0.030})\%$. The angle γ is found to be $\gamma = (65.4^{+3.8}_{-4.2})^\circ$ and is the most precise determination from a single experiment.

KEYWORDS: B physics, Charm physics, CKM angle gamma, CP violation, Hadron-Hadron scattering (experiments)

ARXIV EPRINT: [2110.02350](https://arxiv.org/abs/2110.02350)

Contents

1	Introduction	1
2	Assumptions	6
3	Statistical treatment	7
4	Results	8
5	Conclusion	13
A	Correlation matrix	14
B	Contribution of each input measurement to the global χ^2	17
C	Pull distribution of each input observable	17
D	Additional figures	21
	The LHCb collaboration	26

1 Introduction

Precise measurements of the Cabibbo-Kobayashi-Maskawa (CKM) unitarity triangle provide a strict test of the Standard Model (SM) and allow for indirect new physics searches in the quark sector up to very high mass scales. The CP violating phase $\gamma \equiv \arg[-V_{ud}V_{ub}^*/V_{cd}V_{cb}^*]$, where $V_{qq'}$ is the relevant CKM matrix element, is the only angle of the unitarity triangle that can be determined using solely measurements of tree-level B -meson decays [1–8] with negligible theoretical uncertainty [9], assuming no sizeable new physics effects are present at tree level [10]. Deviations between direct measurements of γ and the value derived from global CKM fits, which assume validity of the SM and hence unitarity of the CKM matrix, would be a clear indication of physics beyond the SM. Furthermore, comparisons between the value of γ measured using decays of different B -meson species provide sensitivity to possible new physics effects at tree level given the different decay topologies involved. The world average for direct measurements of $\gamma = (66.2^{+3.4}_{-3.6})^\circ$ [11] is dominated by LHCb results. The experimental uncertainty on γ is larger than that obtained from global CKM fits, $\gamma = (65.6^{+0.9}_{-2.7})^\circ$ [12] using a frequentist framework, and $\gamma = (65.8 \pm 2.2)^\circ$ [13] with a Bayesian approach. Closing this sensitivity gap is a key physics goal of the LHCb experiment and the comparison between the direct and indirect determinations of γ is an important test of the SM.

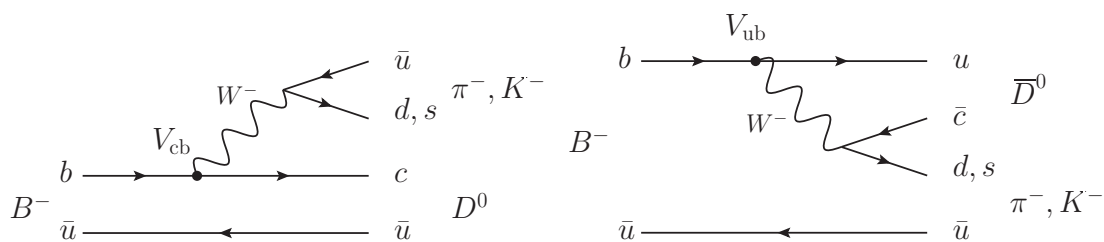


Figure 1. Leading-order Feynman diagrams for $B^- \rightarrow Dh^-$ decays with a (left) favoured $b \rightarrow c$ and (right) suppressed $b \rightarrow u$ quark transition.

The CKM angle γ is measured in decays which are sensitive to interference between favoured $b \rightarrow c$ and suppressed $b \rightarrow u$ quark transition amplitudes that are proportional to V_{cb} and V_{ub} , respectively.¹ The ratio of these two amplitudes is given by $\mathcal{A}_{\text{sup}}/\mathcal{A}_{\text{fav}} = r_B e^{i\delta_B \pm \gamma}$, where the $+$ or $-$ sign indicates whether the initial state contains a \bar{b} - or b -quark, r_B is the ratio of the amplitude magnitudes, and δ_B their CP -conserving strong-phase difference. This interference effect is typically measured in B -meson decays such as $B^\pm \rightarrow Dh^\pm$, where D is an admixture of the D^0 and \bar{D}^0 flavour states, and h^\pm is either a charged kaon or pion. Figure 1 shows the leading-order Feynman diagrams for the favoured and suppressed processes. Interference effects, providing sensitivity to γ , only occur when the D meson decays to a final state, f , accessible to both D^0 and \bar{D}^0 mesons. Neglecting mixing in the neutral charm system, the decay rate for a $B^\pm \rightarrow Dh^\pm$ decay is given by

$$\Gamma(B^\pm \rightarrow Dh^\pm) \propto |r_D e^{-i\delta_D} + r_B e^{i(\delta_B \pm \gamma)}|^2 \Rightarrow r_D^2 + r_B^2 + 2\kappa_D \kappa_B r_D r_B \cos(\delta_B + \delta_D \pm \gamma), \quad (1.1)$$

where r_D and δ_D are the magnitude ratio and strong-phase difference between the $D^0 \rightarrow f$ and $\bar{D}^0 \rightarrow f$ amplitudes. For D decays to CP eigenstates, e.g. $D \rightarrow K^+ K^-$, these values are $r_D = 1$ and $\delta_D = 0$. The coherence factors of B and D decays, κ_B and κ_D , are equal to unity for two-body decays, and account for a dilution of the interference term due to incoherence (strong phase variation) between contributing intermediate resonances in multibody decays. The hadronic parameters, r_B , δ_B , r_D , δ_D , are specific to each B decay and subsequent D decay, respectively. However, the CP -violating weak phase difference between B^+ and B^- amplitudes, γ , is shared by all such decays.

Equation (1.1) has at least five unknown parameters, even more if the coherence factors are not set to unity, hence they cannot be determined using a single pair of B^\pm decay rates. This is overcome by combining the results from many different D -decay modes to overconstrain the parameters of the B -meson decay, provided that the corresponding r_D , δ_D and κ_D parameters are constrained by other measurements. In past combinations these parameters have been taken as external inputs using dedicated charm-meson measurements. The large B -meson samples now constrain γ and δ_B so precisely that $\delta_D^{K\pi}$, the strong phase difference between $D^0 \rightarrow K^- \pi^+$ and $\bar{D}^0 \rightarrow K^- \pi^+$ decays, can be measured with similar precision as γ and δ_B , a factor of about two better than the previous world average [11].

¹Charge conjugation is implied throughout unless stated otherwise.

This improved precision on $\delta_D^{K\pi}$ can then be used to improve knowledge of charm mixing as described below.

The mass eigenstates of the neutral charm mesons can be written as $|D_{1,2}\rangle \equiv p|D^0\rangle \pm q|\bar{D}^0\rangle$, where p and q are complex parameters such that $|p|^2 + |q|^2 = 1$. The D_1 (D_2) state corresponds to the $+$ ($-$) sign and is approximately CP even (odd) in the chosen convention. The mixing of charm flavour states can be described by two dimensionless parameters, $x \equiv (m_1 - m_2)/\Gamma$ and $y \equiv (\Gamma_1 - \Gamma_2)/2\Gamma$, where m_i (Γ_i) is the mass (width) of the appropriate D mass state, and Γ their average decay width.² Effects of CP violation in D^0 and \bar{D}^0 decays to a common final state, f , can be seen in mixing if $|q/p| \neq 1$, or in the interference between mixing and decay if $\phi \equiv \arg(q/p) \neq 0, \pi$.³ Study of the charm mixing parameters is of high interest in its own right, because the flavour-changing neutral currents responsible for the mixing transition do not occur at tree-level in the SM, and thus can be significantly affected by contributions from new heavy particles. The world averages for $x = (4.09^{+0.48}_{-0.49}) \times 10^{-3}$ and $y = (6.15^{+0.56}_{-0.55}) \times 10^{-3}$ [11] are dominated by LHCb results.

The mixing parameters, x and y , can be determined using the ratio of wrong-sign (WS), $D^0 \rightarrow K^+\pi^-$, and right-sign (RS), $D^0 \rightarrow K^-\pi^+$, time-dependent decay rates. This ratio is

$$R^\pm(t) \approx R^\pm + \sqrt{R^\pm} y'^\pm \left(\frac{t}{\tau}\right) + \frac{(x'^\pm)^2 + (y'^\pm)^2}{4} \left(\frac{t}{\tau}\right)^2, \quad (1.2)$$

up to second order in the mixing parameters, where t is the decay time, τ is the D^0 meson lifetime, and the $+$ ($-$) signs correspond to the decay-rate ratio for a flavour-tagged D^0 (\bar{D}^0) initial state.⁴ The parameter $R^\pm = r_D^2(1 \pm A_D)$ is the ratio of suppressed-to-favoured decay rates, modulated by the direct CP asymmetry, A_D , between D^0 and \bar{D}^0 WS decays. The parameters $x'^\pm \equiv -|q/p|^{\pm 1} [x \cos(\delta_D^{K\pi} \pm \phi) + y \sin(\delta_D^{K\pi} \pm \phi)]$ and $y'^\pm \equiv -|q/p|^{\pm 1} [y \cos(\delta_D^{K\pi} \pm \phi) - x \sin(\delta_D^{K\pi} \pm \phi)]$ encode the mixing. Since $\delta_D^{K\pi}$ is close to π and ϕ is almost zero [11], it follows that $R^\pm(t)$ is mostly sensitive to the parameter y through the term linear in decay time and mixing parameters, and currently the precision on y is limited by the precision with which $\delta_D^{K\pi}$ is known. Consequently, a simultaneous combination using both beauty and charm observables from LHCb is performed for the first time, improving the precision on y (x) by about 50% (2%).

A further motivation for the simultaneous combination of both beauty and charm measurements is that non-negligible effects due to charm-meson mixing give rise to additional terms in eq. (1.1). Incorporating the effect of D -meson mixing, up to first order in x and

²Natural units, with $c = \hbar = 1$, are used throughout.

³The Wolfenstein parametrisation and the convention that $CP|D^0\rangle = |\bar{D}^0\rangle$ is used.

⁴It should be noted that there are multiple conventions in the literature for the strong phase $\delta_D^{K\pi}$, depending on whether the discussion involves the CKM angle γ or charm mixing. The convention in which $\delta_D \rightarrow \pi$ in the SU(3) limit is used, which is shifted by π with respect to the convention employed by the HFLAV Charm group.

y , means the decay rate of eq. (1.1) becomes [14]

$$\begin{aligned} \Gamma(B^\pm \rightarrow Dh^\pm) \propto & r_D^2 + r_B^2 + 2\kappa_D \kappa_{BR} r_D r_B \cos(\delta_B + \delta_D \pm \gamma) \\ & - \alpha \left[(1 + r_B^2) \kappa_{DR} r_D \cos(\delta_D) + (1 + r_D^2) \kappa_{BR} r_B \cos(\delta_B \pm \gamma) \right] y \\ & + \alpha \left[(1 - r_B^2) \kappa_{DR} r_D \sin(\delta_D) - (1 - r_D^2) \kappa_{BR} r_B \sin(\delta_B \pm \gamma) \right] x, \end{aligned} \quad (1.3)$$

where the α coefficient accounts for the non-uniform decay-time acceptance of the LHCb detector. For cases where $r_B \gg x, y$, such as the $B^\pm \rightarrow DK^\pm$ decay, the effect of D mixing is small. However, for decays like $B^\pm \rightarrow D\pi^\pm$, where $r_B \sim x, y$, the effect is significant [14]. Studies of this combination, which includes both $B^\pm \rightarrow DK^\pm$ and $B^\pm \rightarrow D\pi^\pm$ modes, suggest that not accounting for the effect of D -meson mixing results in a bias on γ of approximately 1.8° , and an ever larger bias for the hadronic parameters, $r_{B^\pm}^{D\pi^\pm}$ and $\delta_{B^\pm}^{D\pi^\pm}$, of the $B^\pm \rightarrow D\pi^\pm$ system. Thus an unbiased determination of γ, x and y requires the simultaneous combination produced in this article.

This article presents results for the weak phase γ and charm mixing and CP violation parameters $x, y, |q/p|$ and ϕ , as well as for several additional amplitude ratios and strong phases, using data collected at the LHCb experiment during the first two runs of the LHC. The statistical procedure is identical to that described in ref. [15] and follows a frequentist treatment which is described in detail in ref. [16] and briefly recapped in section 3. The results have additionally been cross-checked using Bayesian inference, which finds very similar values. The results presented here supersede previous LHCb combinations [15–18].

The full list of LHCb measurements that are used as inputs to the combination is provided in table 1. In the beauty sector this includes decay-rate ratios and charge asymmetries of $B^\pm \rightarrow Dh^\pm, B^\pm \rightarrow D^*h^\pm, B^\pm \rightarrow DK^{*\pm}, B^\pm \rightarrow Dh^\pm\pi^+\pi^-, B^0 \rightarrow DK^{*0}, B^0 \rightarrow D^\mp\pi^\pm, B_s^0 \rightarrow D_s^\mp K^\pm$ and $B_s^0 \rightarrow D_s^\mp K^\pm\pi^+\pi^-$ decays, where D^* is an admixture of D^{*0} and \bar{D}^{*0} flavour states. In the charm sector this includes time-dependent measurements of $D^0 \rightarrow h^+h^-, D^0 \rightarrow K^+\pi^-, D^0 \rightarrow K^\pm\pi^\mp\pi^+\pi^-$ and $D^0 \rightarrow K_S^0\pi^+\pi^-$ decays. There are seven new or updated measurements from beauty-meson decays since the last combination, including LHCb Run 2 updates from the highly sensitive $B^\pm \rightarrow Dh^\pm$ with $D \rightarrow K_S^0h^+h^-$ [19] and $D \rightarrow h^+h^-$ [20] decays. The eight inputs from LHCb charm analyses are included in the combination for the first time.

Additional external constraints are summarised in table 2; these are used predominantly to provide auxiliary information on the hadronic parameters and coherence factors in multibody B and D decays. In the case of quasi- CP -eigenstate decays, such as $D \rightarrow \pi^+\pi^-\pi^+\pi^-$, the coherence factor is determined by the fraction of CP -even content in the final-state amplitude, $F^+ = (\kappa_D + 1)/2$. In the case of the $B^0 \rightarrow D^\mp\pi^\pm, B_s^0 \rightarrow D_s^\mp K^\pm$ and $B_s^0 \rightarrow D_s^\mp K^\pm\pi^+\pi^-$ modes, the weak phases measured through the time-dependent CP asymmetry are $(\gamma + 2\beta)$ and $(\gamma - 2\beta_s)$, induced via interference between $B_{(s)}^0$ mixing and decay. Therefore, in order to obtain sensitivity to γ , external constraints from the world averages of $\beta \equiv \arg[-V_{cd}V_{cb}^*/V_{td}V_{tb}^*]$ and $\phi_s \approx -2\beta_s \equiv -2 \arg[-V_{ts}V_{tb}^*/V_{cs}V_{cb}^*]$ [11] are included.

<i>B</i> decay	<i>D</i> decay	Ref.	Dataset	Status since Ref. [17]
$B^\pm \rightarrow Dh^\pm$	$D \rightarrow h^+h^-$	[20]	Run 1&2	Updated
$B^\pm \rightarrow Dh^\pm$	$D \rightarrow h^+\pi^-\pi^+\pi^-$	[21]	Run 1	As before
$B^\pm \rightarrow Dh^\pm$	$D \rightarrow h^+h^-\pi^0$	[22]	Run 1	As before
$B^\pm \rightarrow Dh^\pm$	$D \rightarrow K_S^0 h^+h^-$	[19]	Run 1&2	Updated
$B^\pm \rightarrow Dh^\pm$	$D \rightarrow K_S^0 K^\pm \pi^\mp$	[23]	Run 1&2	Updated
$B^\pm \rightarrow D^*h^\pm$	$D \rightarrow h^+h^-$	[20]	Run 1&2	Updated
$B^\pm \rightarrow DK^{*\pm}$	$D \rightarrow h^+h^-$	[24]	Run 1&2(*)	As before
$B^\pm \rightarrow DK^{*\pm}$	$D \rightarrow h^+\pi^-\pi^+\pi^-$	[24]	Run 1&2(*)	As before
$B^\pm \rightarrow Dh^\pm \pi^+ \pi^-$	$D \rightarrow h^+h^-$	[25]	Run 1	As before
$B^0 \rightarrow DK^{*0}$	$D \rightarrow h^+h^-$	[26]	Run 1&2(*)	Updated
$B^0 \rightarrow DK^{*0}$	$D \rightarrow h^+\pi^-\pi^+\pi^-$	[26]	Run 1&2(*)	New
$B^0 \rightarrow DK^{*0}$	$D \rightarrow K_S^0 \pi^+ \pi^-$	[27]	Run 1	As before
$B^0 \rightarrow D^\mp \pi^\pm$	$D^+ \rightarrow K^- \pi^+ \pi^+$	[28]	Run 1	As before
$B_s^0 \rightarrow D_s^\mp K^\pm$	$D_s^+ \rightarrow h^+ h^- \pi^+$	[29]	Run 1	As before
$B_s^0 \rightarrow D_s^\mp K^\pm \pi^+ \pi^-$	$D_s^+ \rightarrow h^+ h^- \pi^+$	[30]	Run 1&2	New
<i>D</i> decay	Observable(s)	Ref.	Dataset	Status since Ref. [17]
$D^0 \rightarrow h^+h^-$	ΔA_{CP}	[31–33]	Run 1&2	New
$D^0 \rightarrow h^+h^-$	y_{CP}	[34]	Run 1	New
$D^0 \rightarrow h^+h^-$	ΔY	[35–38]	Run 1&2	New
$D^0 \rightarrow K^+ \pi^-$ (Single Tag)	$R^\pm, (x'^\pm)^2, y'^\pm$	[39]	Run 1	New
$D^0 \rightarrow K^+ \pi^-$ (Double Tag)	$R^\pm, (x'^\pm)^2, y'^\pm$	[40]	Run 1&2(*)	New
$D^0 \rightarrow K^\pm \pi^\mp \pi^+ \pi^-$	$(x^2 + y^2)/4$	[41]	Run 1	New
$D^0 \rightarrow K_S^0 \pi^+ \pi^-$	x, y	[42]	Run 1	New
$D^0 \rightarrow K_S^0 \pi^+ \pi^-$	$x_{CP}, y_{CP}, \Delta x, \Delta y$	[43]	Run 1	New
$D^0 \rightarrow K_S^0 \pi^+ \pi^-$	$x_{CP}, y_{CP}, \Delta x, \Delta y$	[44]	Run 2	New

Table 1. Measurements used in the combination. Inputs from the charm system appear in the lower part of the table. Those that are new, or that have changed, since the previous combination [17] are highlighted in bold. Measurements denoted by (*) include only a fraction of the Run 2 sample, corresponding to data taken in 2015 and 2016. Where multiple references are cited, measured values are taken from the most recent results, which include information from the others.

Decay	Parameters	Source	Ref.	Status since Ref. [17]
$B^\pm \rightarrow DK^{*\pm}$	$\kappa_{B^\pm}^{DK^{*\pm}}$	LHCb	[24]	As before
$B^0 \rightarrow DK^{*0}$	$\kappa_{B^0}^{DK^{*0}}$	LHCb	[45]	As before
$B^0 \rightarrow D^\mp \pi^\pm$	β	HFLAV	[11]	Updated
$B_s^0 \rightarrow D_s^\mp K^\pm(\pi\pi)$	ϕ_s	HFLAV	[11]	Updated
$D \rightarrow h^+ h^- \pi^0$	$F_{\pi\pi\pi^0}^+, F_{K\pi\pi^0}^+$	CLEO-c	[46]	As before
$D \rightarrow \pi^+ \pi^- \pi^+ \pi^-$	$F_{4\pi}^+$	CLEO-c	[46]	As before
$D \rightarrow K^+ \pi^- \pi^0$	$r_D^{K\pi\pi^0}, \delta_D^{K\pi\pi^0}, \kappa_D^{K\pi\pi^0}$	CLEO-c+LHCb+BESIII	[47–49]	Updated
$D \rightarrow K^\pm \pi^\mp \pi^+ \pi^-$	$r_D^{K3\pi}, \delta_D^{K3\pi}, \kappa_D^{K3\pi}$	CLEO-c+LHCb+BESIII	[41, 47–49]	Updated
$D \rightarrow K_S^0 K^\pm \pi^\mp$	$r_D^{K_S^0 K\pi}, \delta_D^{K_S^0 K\pi}, \kappa_D^{K_S^0 K\pi}$	CLEO	[50]	As before
$D \rightarrow K_S^0 K^\pm \pi^\mp$	$r_D^{K_S^0 K\pi}$	LHCb	[51]	As before

Table 2. Auxiliary inputs used in the combination. Those highlighted in bold have changed since the previous combination [17].

2 Assumptions

The mathematical formulae relating the input observables to the parameters of interest, via eq. (1.3), contain a few assumptions. These are detailed below and their impact on the results has been checked to be negligible at the current precision. In the future, as the precision on γ approaches one degree, many of them will need to be reassessed.

Neutral kaon mixing. The extraction of γ from decays where the final state of the D meson decay contains a neutral kaon is affected by CP violation in $K^0-\bar{K}^0$ mixing and decay and by regeneration [52]. For the $D \rightarrow K_S^0 h^+ h^-$ final state, a relative shift of approximately $\Delta\gamma/\gamma \approx \mathcal{O}(10^{-3})$ is expected; this has been studied in detail in ref. [52]. Furthermore, the result of the relevant input analysis includes a small systematic uncertainty to account for this [19], so these effects are not considered further in this combination. The size of the effect in $D \rightarrow K_S^0 K^\pm \pi^\mp$ final states is larger, $\Delta\gamma/\gamma \approx \mathcal{O}(\varepsilon_K/r_B)$, where $\varepsilon_K = (2.10_{-0.20}^{+0.27}) \times 10^{-3}$ quantifies CP violation in neutral kaon mixing [12]. However, the impact on γ is negligible at present because the sensitivity of the input measurement is relatively low [23].

CP violation in D -meson decays. The effect of CP violation in the direct decay of $D^0 \rightarrow K_S^0 h^+ h^-$ is not considered because it is negligible in the SM for the Cabibbo-favoured (CF) and doubly Cabibbo-suppressed (DCS) amplitudes contributing to that process. However, the effect of CP violation in the direct decay of $D^0 \rightarrow K^+ \pi^-$ is allowed for in the charm part of the combination, and is denoted by A_D . A non-zero value of A_D would cause a small shift in the charge asymmetries measured for $D^0 \rightarrow K^+ \pi^-$ final states in the beauty system, which is not accounted for in this combination. The impact on the determination of γ is found to be smaller than 0.2° . The difference between the size of direct CP violation in $D^0 \rightarrow K^+ K^-$ and $D^0 \rightarrow \pi^+ \pi^-$ decays is included as an input

in the charm part of the fit [31]. In the beauty system, this value is used to account for direct CP violation in $D^0 \rightarrow h^+h^-$ decays for the most sensitive analyses, where the D meson is produced in $B^\pm \rightarrow Dh^\pm$ or $B^\pm \rightarrow D^*h^\pm$ decays, under the hypothesis of U -spin symmetry, $A_{CP}(KK) = -A_{CP}(\pi\pi) = \Delta A_{CP}/2$, where $A_{CP}(f)$ is the CP asymmetry of the D meson decay to the final state f . Any U -spin breaking effects are negligible given that ignoring any direct CP violation in $D \rightarrow h^+h^-$ decays only has a small impact, below 0.3° , on the determination of γ . Time-dependent CP violation in charm mixing, which would add additional terms to eq. (1.3), is also neglected in the beauty system, since its impact on the determination of γ is smaller than 0.1° [14].

Strong phases in $D \rightarrow K_S^0 h^+ h^-$ decays. The input measurements containing $D \rightarrow K_S^0 h^+ h^-$ final states [19, 27, 43, 44], both in the charm and beauty systems, require external knowledge of the strong-phase difference between the $D^0 \rightarrow K_S^0 h^+ h^-$ and $\bar{D}^0 \rightarrow K_S^0 h^+ h^-$ amplitudes across the phase space of the D decay. These values are taken from a combination of CLEO-c and BES-III measurements [53–56] and their uncertainties propagated to the uncertainties of the input measurements listed in table 1. In this combination, each set of input measurements is treated as statistically independent and thus a small part of the already sub-dominant systematic uncertainties of these measurements is being counted twice in the $D \rightarrow K_S^0 \pi^+ \pi^-$ system *i.e.* the appropriate correlation is not accounted for. This correlation is non-trivial to compute owing to the different binning schemes employed by the different input analyses. In any case, the effect on this combination is small since the uncertainty on the strong phases accounts for approximately 0.5° of the uncertainty on γ , 40% of the uncertainty on x and 1% of the uncertainty on y , and these parameters are nearly uncorrelated. Studies suggest that incorporation of this correlation will become important only with a three times larger data sample.

Correlations of systematic uncertainties between input measurements. In addition to the effect of strong phases in $D \rightarrow K_S^0 h^+ h^-$ decays, there are various other potential systematic correlations that are not accounted for. Whilst the individual input analyses provide both statistical and systematic covariance matrices between the sets of observables they measure, there are in principle sub-leading systematic correlations between input analyses which are not accounted for. For example, systematic uncertainties originating from production and detection asymmetries will be correlated for most time-integrated measurements and those originating from knowledge of decay-time acceptance and resolution will be correlated for time-dependent measurements. The impact of ignoring these small correlations is a marginal underestimation of the uncertainties (assuming the correlation is positive), but given that the combination is still statistically dominated (3.3° out of 3.6°) the effect is expected to be negligible.

3 Statistical treatment

The results are obtained using a frequentist treatment, with a likelihood function built from the product of the probability density functions, f_i , of experimental observables \vec{A}_i ,

defined as

$$\mathcal{L}(\vec{\alpha}) = \prod_i f_i(\vec{A}_i^{\text{obs}}|\vec{\alpha}). \quad (3.1)$$

Here, \vec{A}_i^{obs} denotes the measured observables from analysis i , and $\vec{\alpha}$ is the set of underlying physics parameters on which they depend. The observables of each input are assumed to follow a multi-dimensional Gaussian distribution

$$f_i(\vec{A}_i^{\text{obs}}|\vec{\alpha}) \propto \exp\left(-\frac{1}{2}(\vec{A}_i(\vec{\alpha}) - \vec{A}_i^{\text{obs}})^T V_i^{-1} (\vec{A}_i(\vec{\alpha}) - \vec{A}_i^{\text{obs}})\right), \quad (3.2)$$

where V_i is the experimental covariance matrix, including both statistical and systematic uncertainties and their correlations.

A χ^2 -function is defined as $\chi^2(\vec{\alpha}) = -2 \ln \mathcal{L}(\vec{\alpha})$, with the best-fit point given by the global minimum of the χ^2 function, $\chi^2(\vec{\alpha}_{\text{min}})$. The confidence level (CL) for a parameter at a given value, denoted α_0 , is determined in the following way. First, for every fixed α_0 , a new minimum of α' is found, $\chi^2(\vec{\alpha}'_{\text{min}})$, and the deviation from the global minimum, $\Delta\chi^2 = \chi^2(\vec{\alpha}'_{\text{min}}) - \chi^2(\vec{\alpha}_{\text{min}})$, is computed. Second, an ensemble of pseudoexperiments, \vec{A}_j^{MC} , is generated according to the probability distribution of eq. (3.2), with parameters $\vec{\alpha} = \vec{\alpha}'_{\text{min}}$. Finally, for each pseudoexperiment the χ^2 -function is minimised once with the parameter of interest free to vary and once with it at a fixed value α_0 , to obtain the difference, $(\Delta\chi^2)^{\text{MC}}$, from \vec{A}_j^{MC} , in the same way as $\Delta\chi^2$ was computed from \vec{A}_i^{obs} . The p -value, or $1 - \text{CL}$, is then defined as the fraction of pseudoexperiments with $(\Delta\chi^2)^{\text{MC}} > \Delta\chi^2$. This method is often referred to as the $\hat{\mu}$ or *Plugin* method; see ref. [57] for details. Its coverage is not guaranteed [57] for the full parameter space, but can be evaluated at various points across the phase space. The coverage of the intervals quoted in this combination has been computed at several points across the phase space, including at the global minimum, by generating large samples of pseudoexperiments and computing the fraction which contains the generated value within a given confidence level. The coverage of the quoted 68.3% interval for γ is $(67.3 \pm 1.5)\%$, for x is $(68.2 \pm 1.5)\%$, for y is $(67.6 \pm 1.5)\%$, for $|q/p|$ is $(66.6 \pm 1.5)\%$, and for ϕ is $(67.7 \pm 1.5)\%$. Similar coverage is seen for the 95.4% intervals and no correction to the quoted intervals is applied.

4 Results

The combination uses a total of 151 input observables to determine 52 free parameters, and the goodness of fit is found to be 84%, evaluated using the best-fit χ^2 and cross-checked with pseudoexperiments. The resulting confidence intervals for each parameter of interest, except for externally constrained nuisance parameters, are provided in table 3. The correlation matrix of the parameters in table 3 is given in appendix A, tables 7, 8 and 9. The p -value (or $1 - \text{CL}$) distribution as a function of γ is shown in figure 2 for the total combination and for subsets in which the input observables are split by the species of the initial B meson. The corresponding confidence intervals are provided in table 4. Significant differences between initial state B mesons could be an indication of new physics entering at tree-level, as the decay topologies for charged and neutral initial states are different. Figure 2 shows a

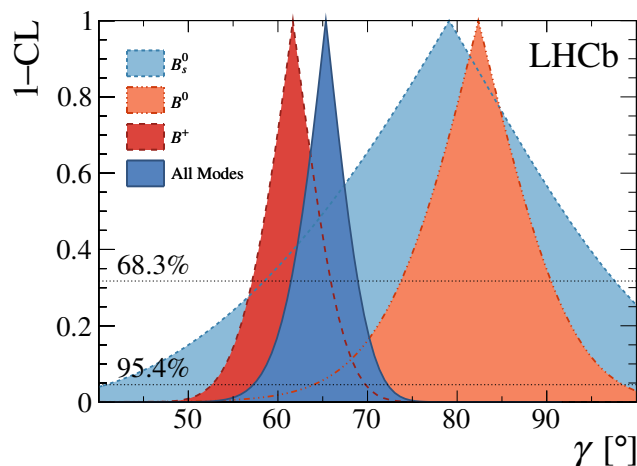


Figure 2. One dimensional 1 – CL profiles for γ from the combination using inputs from B_s^0 (light blue), B^0 (orange), B^+ mesons (red) and all species together (dark blue).

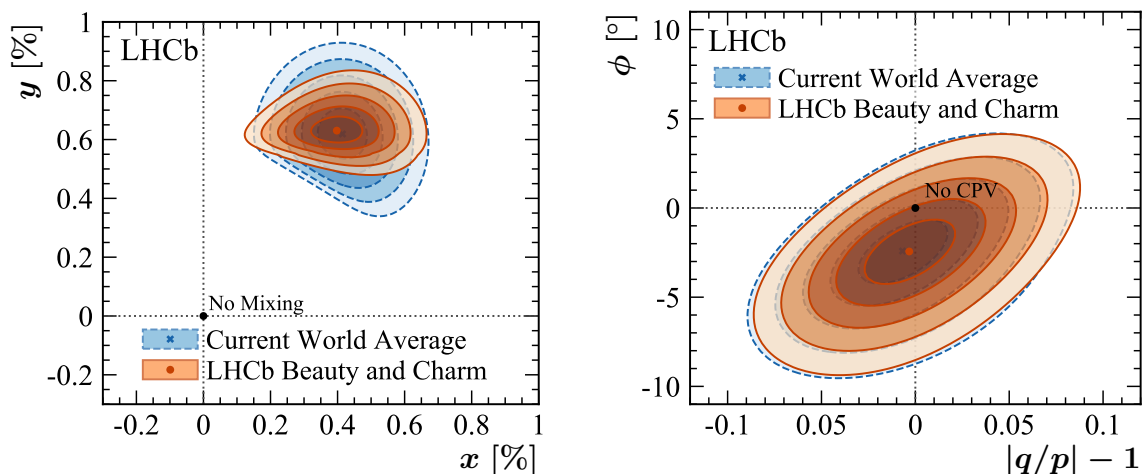


Figure 3. Two-dimensional profile likelihood contours for (left) the charm mixing parameters x and y , and (right) the ϕ and $|q/p|$ parameters. The blue contours show the current charm world average from ref. [11]; the brown contours show the result of this combination. Contours are drawn out from 1 (68.3%) to 5 standard deviations.

moderate tension, 2.2 standard deviations (σ), between the charged and neutral B states. The uncertainties in the B^0 and B_s^0 modes are considerably larger than in the dominant B^+ modes. The sensitivity of the B^0 and B_s^0 modes is expected to improve by approximately a factor of 2 with the analysis of $B^0 \rightarrow DK^+\pi^-$ with $D \rightarrow K_S^0 h^+ h^-$ and $B_s^0 \rightarrow D_s^\mp K^\pm$ decays using the full LHCb data sample. Table 5 presents the confidence intervals for γ as determined from inputs of time-dependent methods and time-integrated methods only. Two-dimensional profile likelihood contours in the (x, y) and $(|q/p|, \phi)$ planes are shown in figure 3. The significant improvement, of a factor of two, in the precision to y demonstrates the advantage of this combination over the current world average in the charm system.

Quantity	Value	68.3% CL		95.4% CL	
		Uncertainty	Interval	Uncertainty	Interval
γ [°]	65.4	+3.8 -4.2	[61.2, 69.2]	+7.5 -8.7	[56.7, 72.9]
$r_{B^\pm}^{DK^\pm}$	0.0984	+0.0027 -0.0026	[0.0958, 0.1011]	+0.0056 -0.0052	[0.0932, 0.1040]
$\delta_{B^\pm}^{DK^\pm}$ [°]	127.6	+4.0 -4.2	[123.4, 131.6]	+7.8 -9.2	[118.4, 135.4]
$r_{B^\pm}^{D\pi^\pm}$	0.00480	+0.00070 -0.00056	[0.00424, 0.00550]	+0.0017 -0.0011	[0.0037, 0.0065]
$\delta_{B^\pm}^{D\pi^\pm}$ [°]	288	+14 -15	[273, 302]	+26 -31	[257, 314]
$r_{B^\pm}^{D^*K^\pm}$	0.099	+0.016 -0.019	[0.080, 0.115]	+0.030 -0.038	[0.061, 0.129]
$\delta_{B^\pm}^{D^*K^\pm}$ [°]	310	+12 -23	[287, 322]	+20 -71	[239, 330]
$r_{B^\pm}^{D^*\pi^\pm}$	0.0095	+0.0085 -0.0061	[0.0034, 0.0180]	+0.017 -0.0089	[0.0006, 0.026]
$\delta_{B^\pm}^{D^*\pi^\pm}$ [°]	139	+22 -86	[53, 161]	+32 -129	[10, 171]
$r_{B^\pm}^{DK^{*\pm}}$	0.106	+0.017 -0.019	[0.087, 0.123]	+0.031 -0.040	[0.066, 0.137]
$\delta_{B^\pm}^{DK^{*\pm}}$ [°]	35	+20 -15	[20, 55]	+57 -28	[7, 92]
$r_{B^0}^{DK^{*0}}$	0.250	+0.023 -0.024	[0.226, 0.273]	+0.044 -0.052	[0.198, 0.294]
$\delta_{B^0}^{DK^{*0}}$ [°]	197	+10 -9.3	[187.7, 207]	+24 -18	[179, 221]
$r_{B^0}^{D_s^\mp K^\pm}$	0.310	+0.098 -0.092	[0.218, 0.408]	+0.20 -0.21	[0.10, 0.51]
$\delta_{B^0}^{D_s^\mp K^\pm}$ [°]	356	+19 -18	[338, 375]	+39 -39	[317, 395]
$r_{B^0}^{D_s^\mp K^\pm \pi^+ \pi^-}$	0.460	+0.081 -0.084	[0.376, 0.541]	+0.16 -0.17	[0.29, 0.62]
$\delta_{B^0}^{D_s^\mp K^\pm \pi^+ \pi^-}$ [°]	345	+13 -12	[333, 358]	+26 -25	[320, 371]
$r_{B^0}^{D^\mp \pi^\pm}$	0.030	+0.014 -0.012	[0.018, 0.044]	+0.036 -0.028	[0.002, 0.066]
$\delta_{B^0}^{D^\mp \pi^\pm}$ [°]	30	+26 -37	[-7, 56]	+45 -81	[-51, 75]
$r_{B^\pm}^{DK^\pm \pi^+ \pi^-}$	0.079	+0.028 -0.034	[0.045, 0.107]	+0.050 -0.079	[0.000, 0.129]*
$r_{B^\pm}^{D\pi^\pm \pi^+ \pi^-}$	0.067	+0.025 -0.029	[0.038, 0.092]	+0.040 -0.067	[0.000, 0.107]*
x [%]	0.400	+0.052 -0.053	[0.347, 0.452]	+0.10 -0.11	[0.29, 0.50]
y [%]	0.630	+0.033 -0.030	[0.600, 0.663]	+0.069 -0.058	[0.572, 0.699]
$r_D^{K\pi}$	0.05867	+0.00015 -0.00015	[0.05852, 0.05882]	+0.00031 -0.00030	[0.05837, 0.05898]
$\delta_D^{K\pi}$ [°]	190.0	+4.2 -4.1	[185.9, 194.2]	+8.6 -8.3	[181.7, 198.6]
$r_D^{K_S^0 K\pi}$	0.6150	+0.0056 -0.0054	[0.6096, 0.6206]	+0.011 -0.011	[0.604, 0.626]
$\delta_D^{K_S^0 K\pi}$ [°]	17	+13 -14	[3, 30]	+26 -30	[-13, 43]
$\kappa_D^{K_S^0 K\pi}$	0.82	± 0.10	[0.72, 0.92]	± 0.20	[0.62, 1.02]
$r_D^{K3\pi}$	0.05560	+0.00059 -0.00058	[0.05502, 0.05619]	+0.0012 -0.0012	[0.0544, 0.0568]
$\delta_D^{K3\pi}$ [°]	154	+15 -16	[138, 169]	+29 -33	[121, 183]
$\kappa_D^{K3\pi}$	0.480	± 0.064	[0.416, 0.544]	± 0.13	[0.35, 0.60]
$ q/p $	0.997	± 0.016	[0.981, 1.013]	± 0.033	[0.964, 1.030]
ϕ [°]	-2.4	± 1.2	[-3.6, -1.2]	± 2.5	[-4.9, 0.1]
$\Delta a_{CP}^{\text{dir}}$	-0.00152	± 0.00029	[-0.00181, -0.00123]	± 0.00058	[-0.00210, -0.00094]

Table 3. Confidence intervals and central values for each of the parameters of interest. Entries marked with an asterisk show where the scan has hit a physical boundary at the lower limit.

Species	Value [°]	68.3% CL		95.4% CL	
		Uncertainty	Interval	Uncertainty	Interval
B^+	61.7	$+4.4$ -4.8	[56.9, 66.1]	$+8.6$ -9.5	[52.2, 70.3]
B^0	82.0	$+8.1$ -8.8	[73.2, 90.1]	$+17$ -18	[64, 99]
B_s^0	79	$+21$ -24	[55, 100]	$+51$ -47	[32, 130]

Table 4. Confidence intervals and best-fit values for γ when splitting the combination inputs by initial B meson species.

Method	Value [°]	68.3% CL		95.4% CL	
		Uncertainty	Interval	Uncertainty	Interval
Time-dependent	79	$+21$ -24	[55, 100]	$+51$ -47	[32, 130]
Time-integrated	64.9	$+3.9$ -4.5	[60.4, 68.8]	$+7.8$ -9.6	[55.3, 72.7]

Table 5. Confidence intervals and best-fit values for γ when splitting the combination inputs by time-dependent and time-integrated methods.

Breakdowns of the contributing components in the combination are shown in figures 4 and 5. These highlight the complementary nature of the input measurements to constrain both γ and the charm mixing parameters. In figure 5 (top left) the dark orange band shows external constraints from CLEO-c [58] and BES-III [59]. These are required to constrain $\delta_D^{K\pi}$ when obtaining the “All Charm Modes” contours, but are not used in the full combination. In the top right and bottom plots the orange bands show the constraints from $D^0 \rightarrow h^+h^-$ modes, but these cannot provide bands in (x, y) or $(|q/p|, \phi)$ without other constraints [60]. Consequently, when these orange bands are produced in the top right plot $(|q/p|, \phi, r_D^{K\pi}, \delta_D^{K\pi})$ are fixed to their best fit values from table 3, while in the bottom plot $(x, y, r_D^{K\pi}, \delta_D^{K\pi})$ are fixed to their best fit values. In the bottom figure the red contour is mostly hidden behind the blue; this is because no significant additional sensitivity to CP violation in the charm system is provided by the inclusion of the beauty observables in the simultaneous fit.

The value of $\gamma = (65.4_{-4.2}^{+3.8})^\circ$ determined from this combination is compatible with, but lower than that of the previous LHCb combination $\gamma = (74_{-5.8}^{+5.0})^\circ$ [17]. This change is driven by improved treatments of background sources in the major inputs described in refs. [19, 20]. An assessment of the compatibility between this and the previous combination, which considers the full parameter space and the correlation between the current set of inputs and the previous set of inputs, finds they are compatible at the level of 2.1σ . The new result is in excellent agreement with the global CKM fit results [12, 13].

The charm mixing parameters, x and y , are determined simultaneously with γ in this combination for the first time. The precision on x is driven by the recent measurement described in ref. [44]. The result $y = (0.630_{-0.030}^{+0.033})\%$ is more precise than the world average, $y = (0.603_{-0.056}^{+0.057})\%$ [11], by approximately a factor of two, driven entirely by the improved measurement of $\delta_D^{K\pi}$ from the beauty system and the simultaneous averaging methodology

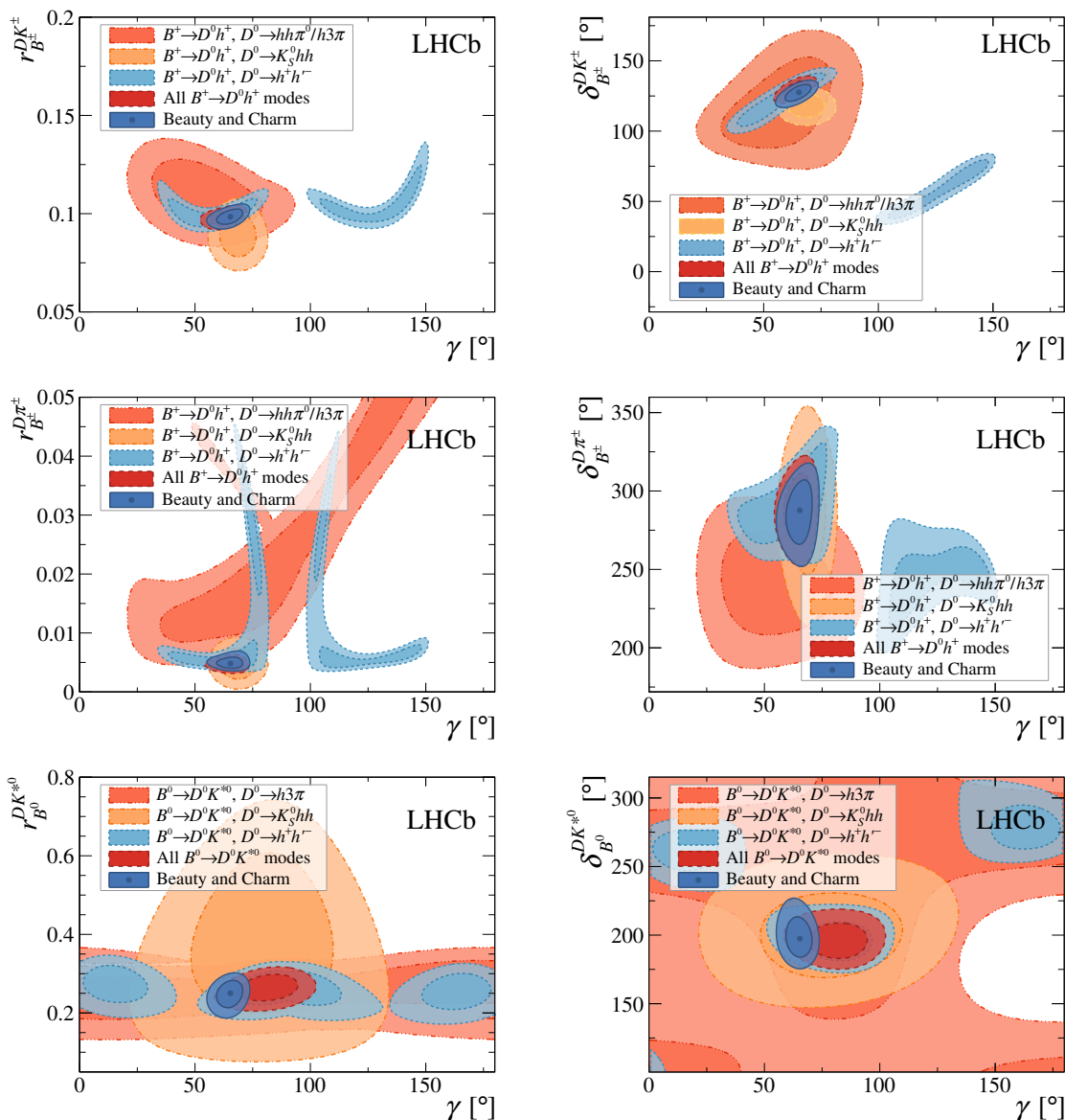


Figure 4. Profile likelihood contours for the beauty decay parameters versus γ , showing the breakdown of sensitivity amongst different sub-combinations of modes. The contours indicate the 68.3% and 95.4% confidence region.

employed in this article. The correlation between $\delta_D^{K\pi}$ and $\delta_{B^\pm}^{DK^\pm}$ is -57% , highlighting $B^\pm \rightarrow DK^\pm$ decays as the source of this improvement.

The beauty part of the combination is cross-checked with an independent framework using a Bayesian statistical treatment. A flat prior is used for γ and the relevant hadronic parameters and results in a value of $\gamma = (65.6_{-3.8}^{+3.7})^\circ$, in agreement with the default frequentist results. Good agreement between the frequentist and Bayesian interpretations is also seen for the other hadronic parameters. A second cross-check using an independent fitting framework with frequentist interpretation gives consistent results to better than

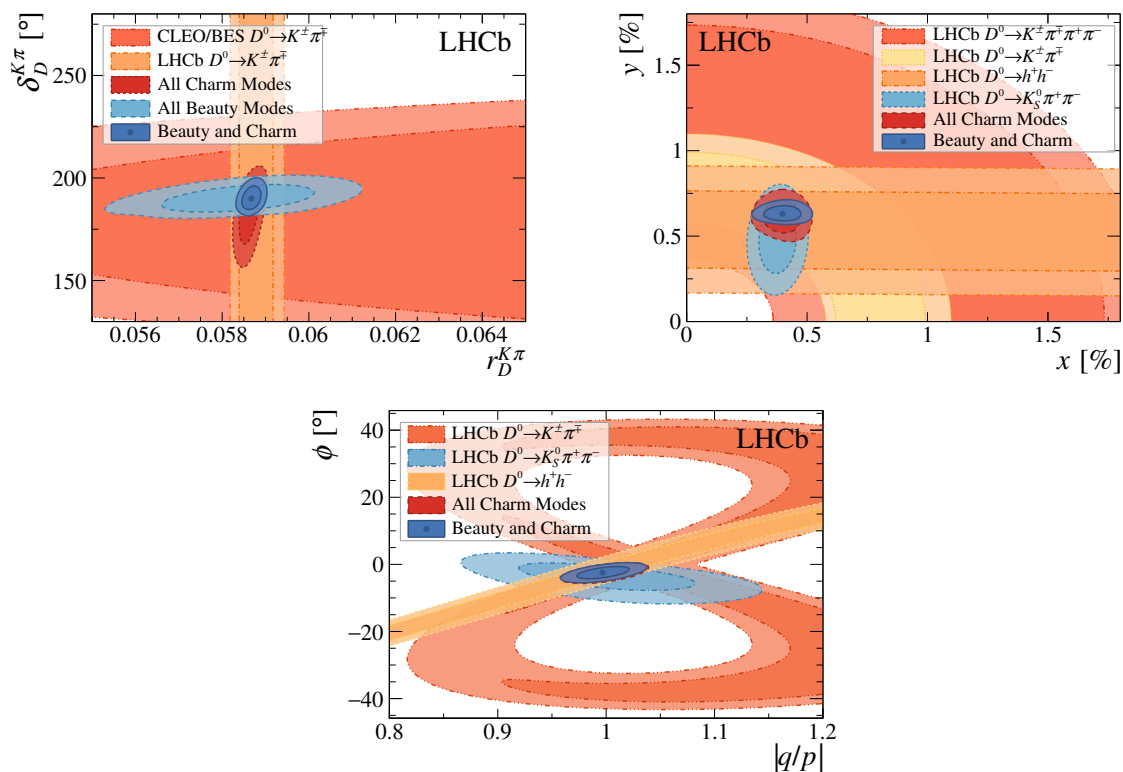


Figure 5. Profile likelihood contours for the charm decay parameters, showing the breakdown of sensitivity amongst different sub-combinations of modes. The contours indicate the 68.3% and 95.4% confidence region.

1% precision. Finally, the charm sector of the combination was validated by accurately reproducing the HFLAV results [11].

The relative impact of systematic uncertainties on the input observables is studied, and found to contribute approximately 1.2° to the result for γ , demonstrating that the uncertainty of this combination is still dominated by the data sample size.

In previous combinations, the experimental input from $B^0 \rightarrow D^\mp \pi^\pm$ decays was included with an external theoretical prediction of $r_{B^0}^{D^\mp \pi^\pm} = 0.0182 \pm 0.0038$ [28]. This prediction assumes SU(3) symmetry, and was the only input from theory. This external input is no longer used, and the combination gives an experimental determination of $r_{B^0}^{D^\mp \pi^\pm} = 0.030^{+0.014}_{-0.012}$. This is in agreement with the theory-based prediction and provides confidence that the assumption of SU(3) symmetry is valid within the current precision. This change has a negligible impact on the determination of other parameters.

5 Conclusion

A simultaneous combination of LHCb measurements sensitive to the CKM angle γ and charm mixing parameters, along with auxiliary information from other experiments, is performed for the first time. This includes seven new and updated inputs from B -meson

decays and eight inputs from D -meson decays. The result,

$$\gamma = (65.4^{+3.8}_{-4.2})^\circ,$$

provides the most precise measurement from a single experiment. The charm mixing parameters are found to be

$$\begin{aligned} x &= (0.400^{+0.052}_{-0.053})\%, \\ y &= (0.630^{+0.033}_{-0.030})\%, \end{aligned}$$

which are the most precise determinations to date. In particular, the uncertainty on y is reduced by a factor of two by using the new procedure described in this paper.

Acknowledgments

We express our gratitude to our colleagues in the CERN accelerator departments for the excellent performance of the LHC. We thank the technical and administrative staff at the LHCb institutes. We acknowledge support from CERN and from the national agencies: CAPES, CNPq, FAPERJ and FINEP (Brazil); MOST and NSFC (China); CNRS/IN2P3 (France); BMBF, DFG and MPG (Germany); INFN (Italy); NWO (Netherlands); MNiSW and NCN (Poland); MEN/IFA (Romania); MSHE (Russia); MICINN (Spain); SNSF and SER (Switzerland); NASU (Ukraine); STFC (United Kingdom); DOE NP and NSF (U.S.A.). We acknowledge the computing resources that are provided by CERN, IN2P3 (France), KIT and DESY (Germany), INFN (Italy), SURF (Netherlands), PIC (Spain), GridPP (United Kingdom), RRCKI and Yandex LLC (Russia), CSCS (Switzerland), IFIN-HH (Romania), CBPF (Brazil), PL-GRID (Poland) and NERSC (U.S.A.). We are indebted to the communities behind the multiple open-source software packages on which we depend. Individual groups or members have received support from ARC and ARDC (Australia); AvH Foundation (Germany); EPLANET, Marie Skłodowska-Curie Actions and ERC (European Union); A*MIDEX, ANR, Labex P2IO and OCEVU, and Région Auvergne-Rhône-Alpes (France); Key Research Program of Frontier Sciences of CAS, CAS PIFI, CAS CCEPP, Fundamental Research Funds for the Central Universities, and Sci. & Tech. Program of Guangzhou (China); RFBR, RSF and Yandex LLC (Russia); GVA, XuntaGal and GENCAT (Spain); the Leverhulme Trust, the Royal Society and UKRI (United Kingdom).

A Correlation matrix

The global fit correlation matrix between each of the parameters presented in table 3 is provided in tables 7, 8 and 9. A subset of this matrix, including only the parameters of greatest interest, is given in table 6. The correlation coefficients for β and ϕ_s are not included as they are almost all smaller than 0.001, an exception is $\rho(\gamma, \phi_s) = -0.009$.

	γ	A_D	$r_D^{K\pi}$	$\delta_D^{K\pi}$	x	y	$ q/p $	ϕ
γ	1.000	—	-0.003	0.003	-0.002	0.003	—	—
A_D		1.000	-0.016	-0.083	-0.003	-0.083	-0.316	0.295
$r_D^{K\pi}$			1.000	0.295	0.282	-0.095	-0.070	0.015
$\delta_D^{K\pi}$				1.000	0.029	0.891	-0.020	0.055
x					1.000	0.013	-0.129	0.083
y						1.000	-0.018	0.040
$ q/p $							1.000	0.554
ϕ								1.000

Table 6. Reduced correlation matrix for the parameters of greater interest. Values smaller than 0.001 are replaced with a — symbol.

	γ	$r_{B^\pm}^{DK^\pm}$	$\delta_{B^\pm}^{DK^\pm}$	$r_{B^\pm}^{D\pi^\pm}$	$\delta_{B^\pm}^{D\pi^\pm}$	$r_{B^\pm}^{D^*K^\pm}$	$\delta_{B^\pm}^{D^*K^\pm}$	$r_{B^\pm}^{D^*\pi^\pm}$	$\delta_{B^\pm}^{D^*\pi^\pm}$	$r_{B^\pm}^{DK^{*\pm}}$	$\delta_{B^\pm}^{DK^{*\pm}}$	$r_{B^0}^{DK^{*0}}$	$\delta_{B^0}^{DK^{*0}}$	$r_{B_s^0}^{D_s^+K^\pm}$
γ	1.000	0.490	0.613	-0.051	0.229	0.138	0.331	0.116	0.149	-0.158	-0.012	0.206	-0.111	-0.003
$r_{B^\pm}^{DK^\pm}$		1.000	0.442	-0.048	0.113	0.058	0.174	0.070	0.100	-0.079	0.026	0.098	-0.047	-0.001
$\delta_{B^\pm}^{DK^\pm}$			1.000	-0.055	0.236	0.062	0.231	0.102	0.156	-0.094	0.054	0.120	-0.052	-0.002
$r_{B^\pm}^{D\pi^\pm}$				1.000	0.629	-0.006	-0.018	-0.008	-0.011	0.006	-0.003	-0.009	0.004	—
$\delta_{B^\pm}^{D\pi^\pm}$					1.000	0.025	0.085	0.034	0.052	-0.035	0.011	0.046	-0.022	—
$r_{B^\pm}^{D^*K^\pm}$						1.000	0.764	-0.211	-0.213	-0.022	-0.006	0.029	-0.016	—
$\delta_{B^\pm}^{D^*K^\pm}$							1.000	-0.172	-0.164	-0.052	0.001	0.067	-0.035	—
$r_{B^\pm}^{D^*\pi^\pm}$								1.000	0.895	-0.018	0.004	0.023	-0.011	—
$\delta_{B^\pm}^{D^*\pi^\pm}$									1.000	-0.023	0.010	0.029	-0.013	—
$r_{B^\pm}^{DK^{*\pm}}$										1.000	-0.323	-0.033	0.017	—
$\delta_{B^\pm}^{DK^{*\pm}}$											1.000	-0.004	0.006	—
$r_{B^0}^{DK^{*0}}$												1.000	-0.139	—
$\delta_{B^0}^{DK^{*0}}$													1.000	—
$r_{B_s^0}^{D_s^+K^\pm}$														1.000

Table 7. Correlation matrix of the fit result, part 1 of 3. Values smaller than 0.001 are replaced with a — symbol.

	$\delta_{B^0}^{D_s^+K^\pm}$	$r_{B^0}^{D_s^+K^\pm\pi^+\pi^-}$	$\delta_{B^0}^{D_s^+K^\pm\pi^+\pi^-}$	$r_{B^0}^{D_s^+\pi^\pm}$	$\delta_{B^0}^{D_s^+\pi^\pm}$	$r_{B^\pm}^{DK^\pm\pi^+\pi^-}$	$r_{B^\pm}^{D\pi^\pm\pi^+\pi^-}$	$r_D^{K\pi}$	$\delta_D^{K\pi}$	x	y	$ q/p $	ϕ
γ	-0.019	-0.027	-0.144	-0.065	-0.168	0.024	-0.181	-0.003	0.003	-0.002	0.003	—	—
$r_{B^\pm}^{DK^\pm}$	-0.009	-0.013	-0.071	-0.032	-0.082	-0.006	0.038	-0.079	-0.236	0.011	-0.206	0.003	-0.010
$\delta_{B^\pm}^{DK^\pm}$	-0.012	-0.017	-0.088	-0.040	-0.103	-0.028	0.196	-0.161	-0.573	0.020	-0.510	0.007	-0.029
$r_{B^\pm}^{D\pi^\pm}$	—	0.001	0.007	0.003	0.009	—	-0.003	0.084	0.022	-0.005	-0.004	-0.005	-0.004
$\delta_{B^\pm}^{D\pi^\pm}$	-0.004	-0.006	-0.033	-0.015	-0.038	-0.007	0.048	0.048	-0.169	—	-0.180	-0.004	-0.016
$r_{B^\pm}^{D^*K^\pm}$	-0.003	-0.004	-0.020	-0.009	-0.023	0.006	-0.046	0.013	0.040	-0.002	0.035	—	0.002
$\delta_{B^\pm}^{D^*K^\pm}$	-0.006	-0.009	-0.048	-0.022	-0.055	0.004	-0.034	-0.012	-0.048	—	-0.044	—	-0.003
$r_{B^\pm}^{D^*\pi^\pm}$	-0.002	-0.003	-0.017	-0.008	-0.019	-0.001	0.008	-0.024	-0.053	0.002	-0.045	0.001	-0.002
$\delta_{B^\pm}^{D^*\pi^\pm}$	-0.003	-0.004	-0.021	-0.010	-0.025	-0.005	0.033	-0.039	-0.112	0.004	-0.097	0.002	-0.005
$r_{B^\pm}^{DK^{*\pm}}$	0.003	0.004	0.023	0.010	0.026	-0.004	0.032	-0.003	-0.006	-0.002	-0.005	—	—
$\delta_{B^\pm}^{DK^{*\pm}}$	—	—	0.002	—	0.002	-0.008	0.057	-0.027	-0.102	0.011	-0.091	—	-0.004
$r_{B^0}^{DK^{*0}}$	-0.004	-0.006	-0.030	-0.013	-0.034	0.006	-0.043	0.002	0.011	-0.002	0.010	—	—
$\delta_{B^0}^{DK^{*0}}$	0.002	0.003	0.016	0.007	0.019	-0.005	0.035	-0.007	-0.028	0.002	-0.025	—	-0.001
$r_{B_s^0}^{D_s^+K^\pm}$	-0.034	—	—	—	—	—	—	—	—	—	—	—	—

Table 8. Correlation matrix of the fit result, part 2 of 3. Values smaller than 0.001 are replaced with a — symbol.

	$\delta_{B_s^0}^{D_s^+ K^\pm}$	$r_{B_s^0}^{D_s^+ K^\pm \pi^+ \pi^-}$	$\delta_{B_s^0}^{D_s^+ K^\pm \pi^+ \pi^-}$	$r_{B^0}^{D^+ \pi^\pm}$	$\delta_{B^0}^{D^+ \pi^\pm}$	$r_{B^\pm}^{DK^\pm \pi^+ \pi^-}$	$r_{B^\pm}^{D\pi^\pm \pi^+ \pi^-}$	$r_D^{K\pi}$	$\delta_D^{K\pi}$	x	y	$ q/p $	ϕ
$\delta_{B_s^0}^{D_s^+ K^\pm}$	1.000	—	0.003	0.001	0.003	—	0.003	—	—	—	—	—	—
$r_{B_s^0}^{D_s^+ K^\pm \pi^+ \pi^-}$		1.000	0.006	0.002	0.005	—	0.005	—	—	—	—	—	—
$\delta_{B_s^0}^{D_s^+ K^\pm \pi^+ \pi^-}$			1.000	0.009	0.024	-0.003	0.026	—	—	—	—	—	—
$r_{B^0}^{D^+ \pi^\pm}$				1.000	0.485	-0.002	0.012	—	—	—	—	—	—
$\delta_{B^0}^{D^+ \pi^\pm}$					1.000	-0.004	0.030	—	—	—	—	—	—
$r_{B^\pm}^{DK^\pm \pi^+ \pi^-}$						1.000	-0.044	0.020	0.074	-0.003	0.066	—	0.004
$r_{B^\pm}^{D\pi^\pm \pi^+ \pi^-}$							1.000	-0.148	-0.531	0.025	-0.473	0.005	-0.026
$r_D^{K\pi}$								1.000	0.295	0.282	-0.095	-0.070	0.015
$\delta_D^{K\pi}$									1.000	0.029	0.892	-0.020	0.055
x										1.000	0.013	-0.129	0.083
y											1.000	-0.018	0.040
$ q/p $												1.000	0.554
ϕ													1.000

Table 9. Correlation matrix of the fit result, part 3 of 3. Values smaller than 0.001 are replaced with a — symbol.

	Measurement	χ^2	No. of obs.
Beauty sector	$B^\pm \rightarrow Dh^\pm, D \rightarrow h^\pm h'^\mp$	2.71	8
	$B^\pm \rightarrow Dh^\pm, D \rightarrow h^\pm \pi^\mp \pi^+ \pi^-$	7.36	8
	$B^\pm \rightarrow Dh^\pm, D \rightarrow h^\pm h'^\mp \pi^0$	7.14	11
	$B^\pm \rightarrow Dh^\pm, D \rightarrow K_S^0 h^+ h^-$	4.67	6
	$B^\pm \rightarrow Dh^\pm, D \rightarrow K_S^0 K^\pm \pi^\mp$	7.57	7
	$B^\pm \rightarrow D^* h^\pm, D \rightarrow h^\pm h'^\mp$	7.31	16
	$B^\pm \rightarrow DK^{*\pm}, D \rightarrow h^\pm h'^\mp (\pi^+ \pi^-)$	3.71	12
	$B^0 \rightarrow DK^{*0}, D \rightarrow h^\pm h'^\mp (\pi^+ \pi^-)$	9.45	12
	$B^0 \rightarrow DK^{*0}, D \rightarrow K_S^0 h^+ h^-$	3.26	4
	$B^\pm \rightarrow Dh^\pm \pi^+ \pi^-, D \rightarrow h^\pm h'^\mp$	1.34	11
	$B_s^0 \rightarrow D_s^\mp K^\pm$	5.71	5
	$B_s^0 \rightarrow D_s^\mp K^\pm \pi^+ \pi^-$	2.88	5
	$B^0 \rightarrow D^\mp \pi^\pm$	0.00	2
Charm sector	$D \rightarrow K_S^0 \pi^+ \pi^-$ 2011	5.38	2
	$D \rightarrow K_S^0 \pi^+ \pi^-$ Run 1	0.77	4
	$D \rightarrow K_S^0 \pi^+ \pi^-$ Run 2	1.37	4
	$D \rightarrow K^\pm \pi^\mp$ Run 1	1.29	6
	$D \rightarrow h^+ h^- \Delta A_{CP}$	0.00	2
	$D \rightarrow K^\pm \pi^\mp \pi^+ \pi^-$	3.59	1
	$D \rightarrow h^+ h^- y_{CP}$	0.40	1
	$D \rightarrow h^+ h^- \Delta Y$	0.15	1
	$D \rightarrow K^\pm \pi^\mp$ Run 2	2.23	6
External constraints	$D \rightarrow K^\pm \pi^\mp \pi^0, D \rightarrow K^\pm \pi^\mp \pi^+ \pi^-$	0.79	6
	$D \rightarrow \pi^+ \pi^- \pi^+ \pi^-$	0.03	1
	$D \rightarrow h^+ h^- \pi^0$	0.01	2
	$D \rightarrow K_S^0 K^\pm \pi^\mp$ WS	0.60	1
	$D \rightarrow K_S^0 K^\pm \pi^\mp$	3.79	3
	$B^\pm \rightarrow DK^{*\pm}$	0.02	1
	$B^0 \rightarrow DK^{*0}$	0.01	1
	ϕ_s	0.00	1
β	0.00	1	
	Total	83.53	151

Table 10. Contributions to the total χ^2 and the number of observables of each input measurement.

B Contribution of each input measurement to the global χ^2

The contribution of each input measurement to the global χ^2 is shown in table 10.

C Pull distribution of each input observable

The pull of each input observable with respect to the global best fit point is shown in figures 6–8. The pull is defined as $(A_{\text{exp}} - A_{\text{fit}})/\sigma(A_{\text{exp}})$, where A_{exp} and A_{fit} are the

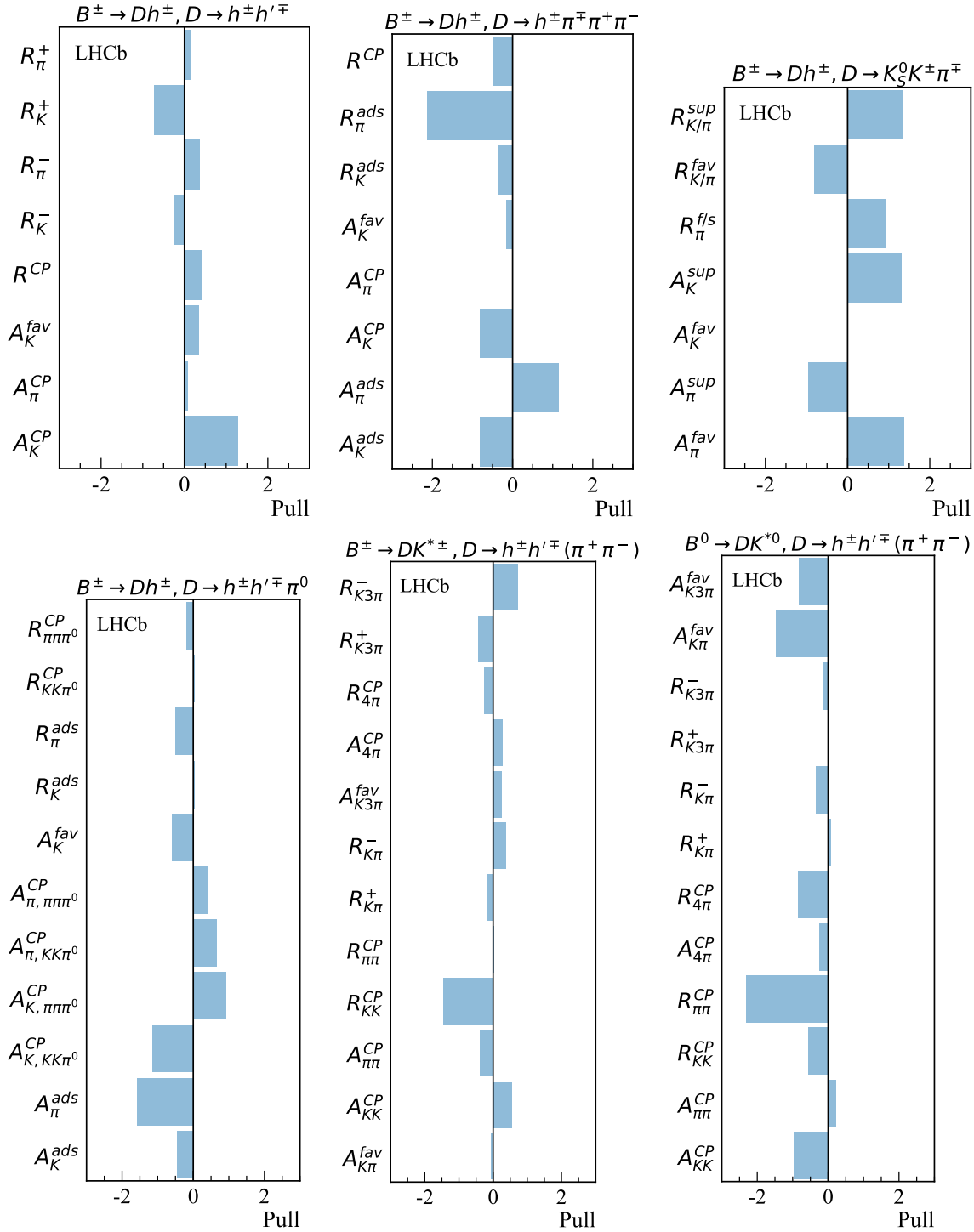


Figure 6. Pulls of the input observables, part 1 of 3.

experimental input value and value at the best-fit point, respectively, and $\sigma(A_{\text{exp}})$ is the experimental uncertainty.

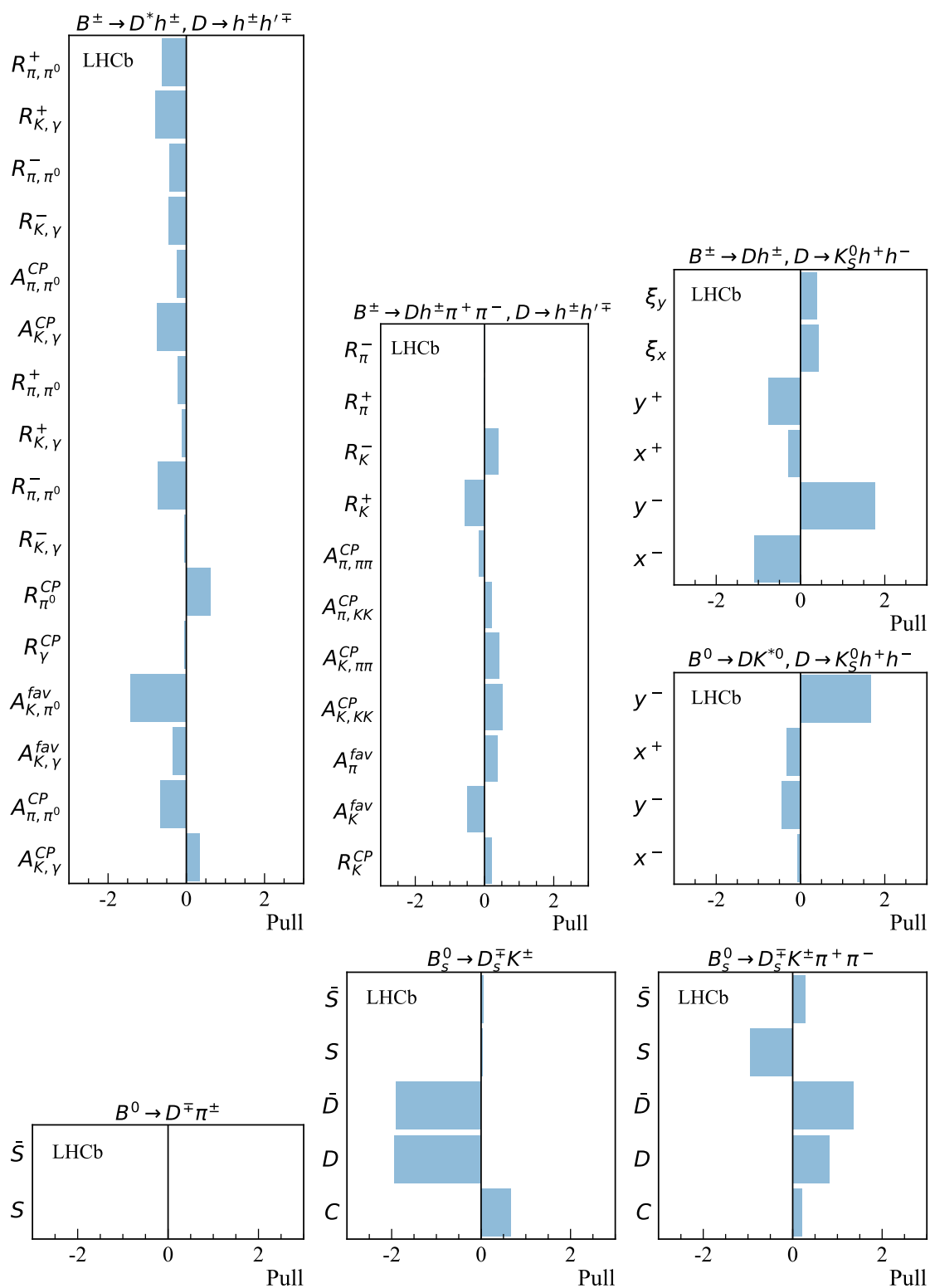


Figure 7. Pulls of the input observables, part 2 of 3.

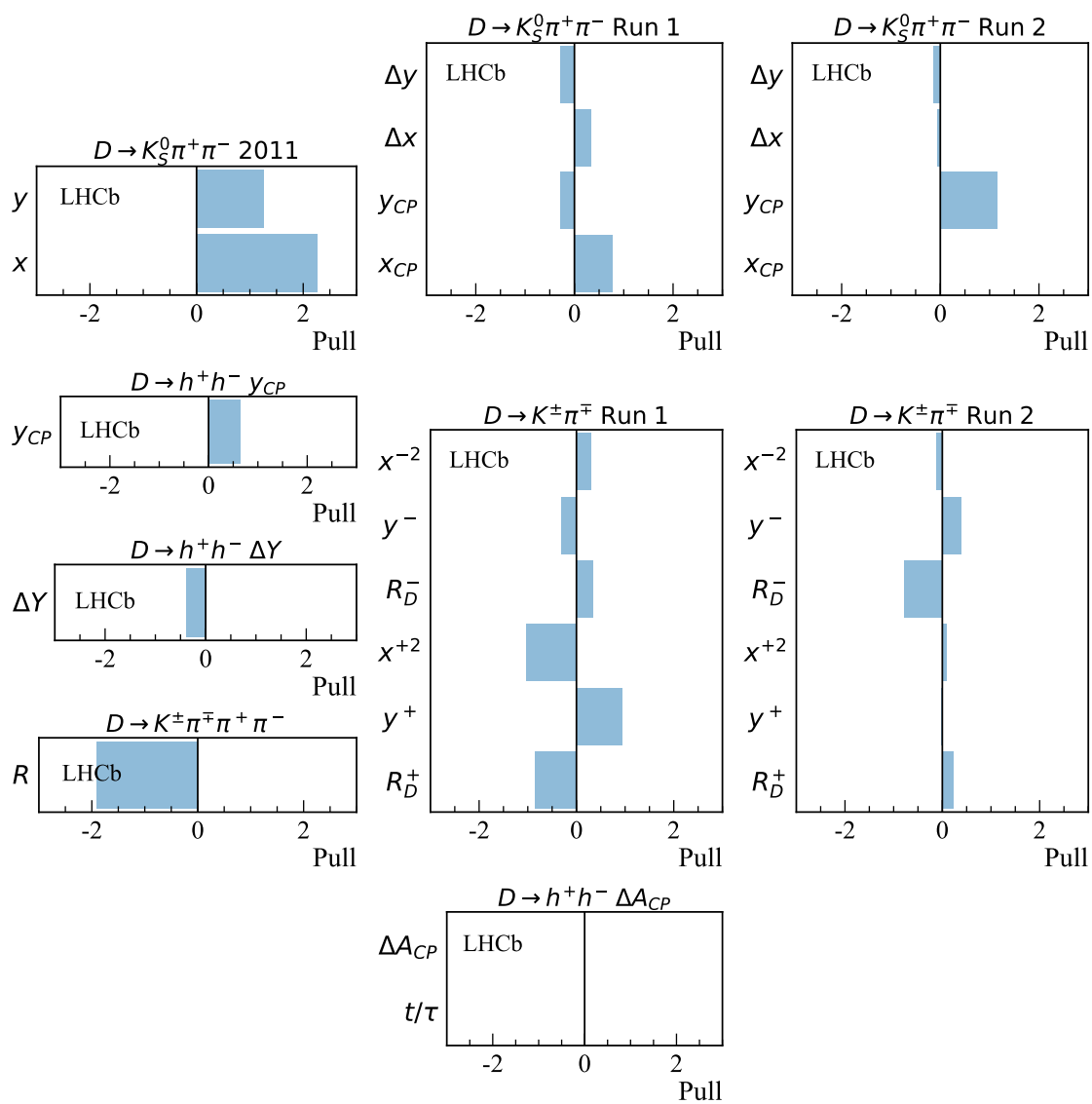


Figure 8. Pulls of the input observables, part 3 of 3.

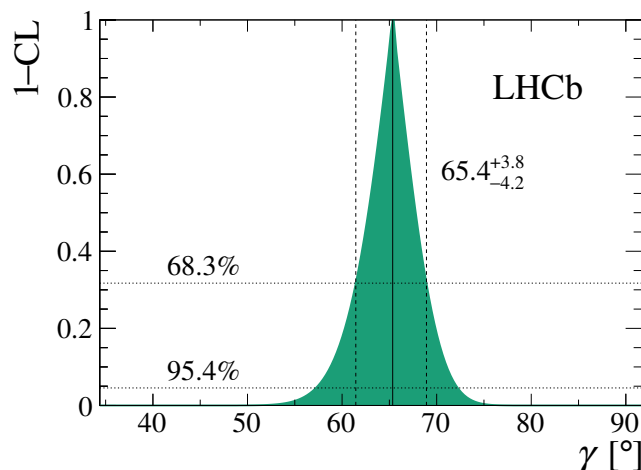


Figure 9. One dimensional $1 - \text{CL}$ profile for γ from all inputs used in the combination.

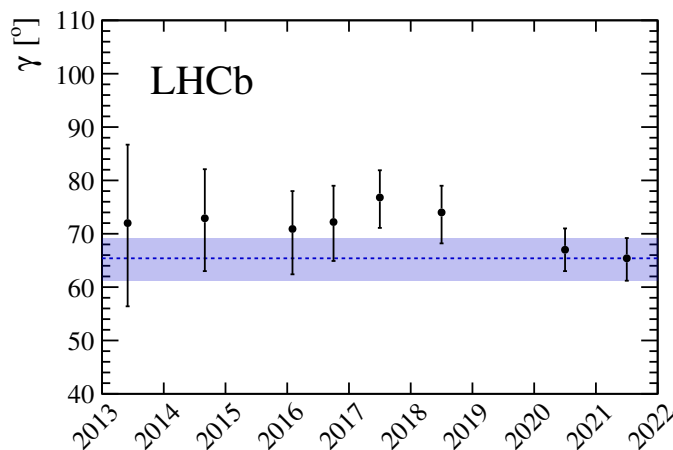


Figure 10. Evolution of the LHCb combination result for γ , with the central values and 1σ uncertainties in black. This result is the 2021 data point, the value and uncertainty are highlighted by the dashed blue line and band, respectively.

D Additional figures

Figure 9 shows the p -value distribution as a function of γ for the global fit. A summary of LHCb γ combination results as a function of time is given in figure 10.

Open Access. This article is distributed under the terms of the Creative Commons Attribution License ([CC-BY 4.0](https://creativecommons.org/licenses/by/4.0/)), which permits any use, distribution and reproduction in any medium, provided the original author(s) and source are credited.

References

- [1] M. Gronau and D. Wyler, *On determining a weak phase from CP asymmetries in charged B decays*, *Phys. Lett. B* **265** (1991) 172 [INSPIRE].
- [2] M. Gronau and D. London, *How to determine all the angles of the unitarity triangle from $B_d^0 \rightarrow DK_s$ and $B_s^0 \rightarrow D^0$* , *Phys. Lett. B* **253** (1991) 483 [INSPIRE].
- [3] D. Atwood, I. Dunietz and A. Soni, *Enhanced CP-violation with $B \rightarrow KD^0(\bar{D}^0)$ modes and extraction of the CKM angle γ* , *Phys. Rev. Lett.* **78** (1997) 3257 [hep-ph/9612433] [INSPIRE].
- [4] D. Atwood, I. Dunietz and A. Soni, *Improved methods for observing CP-violation in $B^\pm \rightarrow KD$ and measuring the CKM phase γ* , *Phys. Rev. D* **63** (2001) 036005 [hep-ph/0008090] [INSPIRE].
- [5] A. Bondar, *Proceedings of BINP special analysis meeting on Dalitz analysis*, unpublished, 24–26 September 2002.
- [6] A. Giri, Y. Grossman, A. Soffer and J. Zupan, *Determining γ using $B^\pm \rightarrow DK^\pm$ with multibody D decays*, *Phys. Rev. D* **68** (2003) 054018 [hep-ph/0303187] [INSPIRE].
- [7] BELLE collaboration, *Measurement of ϕ_3 with Dalitz plot analysis of $B^\pm \rightarrow D^{(*)}K^\pm$ decay*, *Phys. Rev. D* **70** (2004) 072003 [hep-ex/0406067] [INSPIRE].
- [8] Y. Grossman, Z. Ligeti and A. Soffer, *Measuring γ in $B^\pm \rightarrow K^\pm(KK^*)_D$ decays*, *Phys. Rev. D* **67** (2003) 071301 [hep-ph/0210433] [INSPIRE].
- [9] J. Brod and J. Zupan, *The ultimate theoretical error on γ from $B \rightarrow DK$ decays*, *JHEP* **01** (2014) 051 [arXiv:1308.5663] [INSPIRE].
- [10] J. Brod, A. Lenz, G. Tetlalmatzi-Xolocotzi and M. Wiebusch, *New physics effects in tree-level decays and the precision in the determination of the quark mixing angle γ* , *Phys. Rev. D* **92** (2015) 033002 [arXiv:1412.1446] [INSPIRE].
- [11] HFLAV collaboration, *Averages of b-hadron, c-hadron, and τ -lepton properties as of 2018*, *Eur. Phys. J. C* **81** (2021) 226 [arXiv:1909.12524] [INSPIRE].
- [12] J. Charles et al., *Current status of the Standard Model CKM fit and constraints on $\Delta F = 2$ new physics*, *Phys. Rev. D* **91** (2015) 073007 [arXiv:1501.05013] [INSPIRE].
- [13] UTFIT collaboration, *The unitarity triangle fit in the standard model and hadronic parameters from lattice QCD: a reappraisal after the measurements of Δm_s and $BR(B \rightarrow \tau\nu_\tau)$* , *JHEP* **10** (2006) 081 [hep-ph/0606167] [INSPIRE].
- [14] M. Rama, *Effect of D - \bar{D} mixing in the extraction of gamma with $B^- \rightarrow D^0 K^-$ and $B^- \rightarrow D^0 \pi^-$ decays*, *Phys. Rev. D* **89** (2014) 014021 [arXiv:1307.4384] [INSPIRE].
- [15] LHCb collaboration, *Measurement of the CKM angle γ from a combination of LHCb results*, *JHEP* **12** (2016) 087 [arXiv:1611.03076] [INSPIRE].
- [16] LHCb collaboration, *Measurement of the CKM angle γ from a combination of $B^\pm \rightarrow Dh^\pm$ analyses*, *Phys. Lett. B* **726** (2013) 151 [arXiv:1305.2050] [INSPIRE].
- [17] LHCb collaboration, *Update of the LHCb combination of the CKM angle γ* , Tech. Rep. LHCb-CONF-2018-002, CERN, Geneva, Switzerland (2018) [CERN-LHCb-CONF-2018-002].
- [18] LHCb collaboration, *Updated LHCb combination of the CKM angle γ* , Tech. Rep. LHCb-CONF-2020-003, CERN, Geneva, Switzerland (2020) [CERN-LHCb-CONF-2020-003].

- [19] LHCb collaboration, *Measurement of the CKM angle γ in $B^\pm \rightarrow DK^\pm$ and $B^\pm \rightarrow D\pi^\pm$ decays with $D \rightarrow K_S^0 h^+ h^-$* , *JHEP* **02** (2021) 169 [[arXiv:2010.08483](#)] [[INSPIRE](#)].
- [20] LHCb collaboration, *Measurement of CP observables in $B^\pm \rightarrow D^{(*)}K^\pm$ and $B^\pm \rightarrow D^{(*)}\pi^\pm$ decays using two-body D final states*, *JHEP* **04** (2021) 081 [[arXiv:2012.09903](#)] [[INSPIRE](#)].
- [21] LHCb collaboration, *Measurement of CP observables in $B^\pm \rightarrow DK^\pm$ and $B^\pm \rightarrow D\pi^\pm$ with two- and four-body D decays*, *Phys. Lett. B* **760** (2016) 117 [[arXiv:1603.08993](#)] [[INSPIRE](#)].
- [22] LHCb collaboration, *A study of CP violation in $B^\mp \rightarrow Dh^\mp$ ($h = K, \pi$) with the modes $D \rightarrow K^\mp \pi^\pm \pi^0$, $D \rightarrow \pi^+ \pi^- \pi^0$ and $D \rightarrow K^+ K^- \pi^0$* , *Phys. Rev. D* **91** (2015) 112014 [[arXiv:1504.05442](#)] [[INSPIRE](#)].
- [23] LHCb collaboration, *Measurement of CP observables in $B^\pm \rightarrow DK^\pm$ and $B^\pm \rightarrow D\pi^\pm$ with $D \rightarrow K_S^0 K^\pm \pi^\mp$ decays*, *JHEP* **06** (2020) 058 [[arXiv:2002.08858](#)] [[INSPIRE](#)].
- [24] LHCb collaboration, *Measurement of CP observables in $B^\pm \rightarrow DK^{*\pm}$ decays using two- and four-body D final states*, *JHEP* **11** (2017) 156 [Erratum *ibid.* **05** (2018) 067] [[arXiv:1709.05855](#)] [[INSPIRE](#)].
- [25] LHCb collaboration, *Study of $B^- \rightarrow DK^- \pi^+ \pi^-$ and $B^- \rightarrow D\pi^- \pi^+ \pi^-$ decays and determination of the CKM angle γ* , *Phys. Rev. D* **92** (2015) 112005 [[arXiv:1505.07044](#)] [[INSPIRE](#)].
- [26] LHCb collaboration, *Measurement of CP observables in the process $B^0 \rightarrow DK^{*0}$ with two- and four-body D decays*, *JHEP* **08** (2019) 041 [[arXiv:1906.08297](#)] [[INSPIRE](#)].
- [27] LHCb collaboration, *Measurement of the CKM angle γ using $B^0 \rightarrow DK^{*0}$ with $D \rightarrow K_S^0 \pi^+ \pi^-$ decays*, *JHEP* **08** (2016) 137 [[arXiv:1605.01082](#)] [[INSPIRE](#)].
- [28] LHCb collaboration, *Measurement of CP violation in $B^0 \rightarrow D^\mp \pi^\pm$ decays*, *JHEP* **06** (2018) 084 [[arXiv:1805.03448](#)] [[INSPIRE](#)].
- [29] LHCb collaboration, *Measurement of CP asymmetry in $B_s^0 \rightarrow D_s^\mp K^\pm$ decays*, *JHEP* **03** (2018) 059 [[arXiv:1712.07428](#)] [[INSPIRE](#)].
- [30] LHCb collaboration, *Measurement of the CKM angle γ and B_s^0 - \bar{B}_s^0 mixing frequency with $B_s^0 \rightarrow D_s^\mp h^\pm \pi^\pm \pi^\mp$ decays*, *JHEP* **03** (2021) 137 [[arXiv:2011.12041](#)] [[INSPIRE](#)].
- [31] LHCb collaboration, *Observation of CP-violation in charm decays*, *Phys. Rev. Lett.* **122** (2019) 211803 [[arXiv:1903.08726](#)] [[INSPIRE](#)].
- [32] LHCb collaboration, *Measurement of CP asymmetry in $D^0 \rightarrow K^- K^+$ and $D^0 \rightarrow \pi^- \pi^+$ decays*, *JHEP* **07** (2014) 041 [[arXiv:1405.2797](#)] [[INSPIRE](#)].
- [33] LHCb collaboration, *Measurement of the difference of time-integrated CP asymmetries in $D^0 \rightarrow K^- K^+$ and $D^0 \rightarrow \pi^- \pi^+$ decays*, *Phys. Rev. Lett.* **116** (2016) 191601 [[arXiv:1602.03160](#)] [[INSPIRE](#)].
- [34] LHCb collaboration, *Measurement of the charm-mixing parameter y_{CP}* , *Phys. Rev. Lett.* **122** (2019) 011802 [[arXiv:1810.06874](#)] [[INSPIRE](#)].
- [35] LHCb collaboration, *Measurement of indirect CP asymmetries in $D^0 \rightarrow K^- K^+$ and $D^0 \rightarrow \pi^- \pi^+$ decays using semileptonic B decays*, *JHEP* **04** (2015) 043 [[arXiv:1501.06777](#)] [[INSPIRE](#)].
- [36] LHCb collaboration, *Measurement of the CP violation parameter A_Γ in $D^0 \rightarrow K^+ K^-$ and $D^0 \rightarrow \pi^+ \pi^-$ decays*, *Phys. Rev. Lett.* **118** (2017) 261803 [[arXiv:1702.06490](#)] [[INSPIRE](#)].

- [37] LHCb collaboration, *Updated measurement of decay-time-dependent CP asymmetries in $D^0 \rightarrow K^+K^-$ and $D^0 \rightarrow \pi^+\pi^-$ decays*, *Phys. Rev. D* **101** (2020) 012005 [[arXiv:1911.01114](#)] [[INSPIRE](#)].
- [38] LHCb collaboration, *Search for time-dependent CP violation in $D^0 \rightarrow K^+K^-$ and $D^0 \rightarrow \pi^+\pi^-$ decays*, *Phys. Rev. D* **104** (2021) 072010 [[arXiv:2105.09889](#)] [[INSPIRE](#)].
- [39] LHCb collaboration, *Measurements of charm mixing and CP violation using $D^0 \rightarrow K^\pm\pi^\mp$ decays*, *Phys. Rev. D* **95** (2017) 052004 [Erratum *ibid.* **96** (2017) 099907] [[arXiv:1611.06143](#)] [[INSPIRE](#)].
- [40] LHCb collaboration, *Updated determination of D^0 - \bar{D}^0 mixing and CP-violation parameters with $D^0 \rightarrow K^+\pi^-$ decays*, *Phys. Rev. D* **97** (2018) 031101 [[arXiv:1712.03220](#)] [[INSPIRE](#)].
- [41] LHCb collaboration, *First observation of D^0 - \bar{D}^0 oscillations in $D^0 \rightarrow K^+\pi^-\pi^+\pi^-$ decays and measurement of the associated coherence parameters*, *Phys. Rev. Lett.* **116** (2016) 241801 [[arXiv:1602.07224](#)] [[INSPIRE](#)].
- [42] LHCb collaboration, *Model-independent measurement of mixing parameters in $D^0 \rightarrow K_S^0\pi^+\pi^-$ decays*, *JHEP* **04** (2016) 033 [[arXiv:1510.01664](#)] [[INSPIRE](#)].
- [43] LHCb collaboration, *Measurement of the mass difference between neutral charm-meson eigenstates*, *Phys. Rev. Lett.* **122** (2019) 231802 [[arXiv:1903.03074](#)] [[INSPIRE](#)].
- [44] LHCb collaboration, *Observation of the mass difference between neutral charm-meson eigenstates*, *Phys. Rev. Lett.* **127** (2021) 111801 [[arXiv:2106.03744](#)] [[INSPIRE](#)].
- [45] LHCb collaboration, *Constraints on the unitarity triangle angle γ from Dalitz plot analysis of $B^0 \rightarrow DK^+\pi^-$ decays*, *Phys. Rev. D* **93** (2016) 112018 [Erratum *ibid.* **94** (2016) 079902] [[arXiv:1602.03455](#)] [[INSPIRE](#)].
- [46] S. Malde et al., *First determination of the CP content of $D \rightarrow \pi^+\pi^-\pi^+\pi^-$ and updated determination of the CP contents of $D \rightarrow \pi^+\pi^-\pi^0$ and $D \rightarrow K^+K^-\pi^0$* , *Phys. Lett. B* **747** (2015) 9 [[arXiv:1504.05878](#)] [[INSPIRE](#)].
- [47] J. Libby et al., *New determination of the $D^0 \rightarrow K^-\pi^+\pi^0$ and $D^0 \rightarrow K^-\pi^+\pi^+\pi^-$ coherence factors and average strong-phase differences*, *Phys. Lett. B* **731** (2014) 197 [[arXiv:1401.1904](#)] [[INSPIRE](#)].
- [48] T. Evans, S. Harnew, J. Libby, S. Malde, J. Rademacker and G. Wilkinson, *Improved determination of the $D \rightarrow K^-\pi^+\pi^+\pi^-$ coherence factor and associated hadronic parameters from a combination of $e^+e^- \rightarrow \psi(3770) \rightarrow c\bar{c}$ and $pp \rightarrow c\bar{c}X$ data*, *Phys. Lett. B* **757** (2016) 520 [Erratum *ibid.* **765** (2017) 402] [[arXiv:1602.07430](#)] [[INSPIRE](#)].
- [49] BESIII collaboration, *Measurement of the $D \rightarrow K^-\pi^+\pi^+\pi^-$ and $D \rightarrow K^-\pi^+\pi^0$ coherence factors and average strong-phase differences in quantum-correlated $D\bar{D}$ decays*, *JHEP* **05** (2021) 164 [[arXiv:2103.05988](#)] [[INSPIRE](#)].
- [50] CLEO collaboration, *Studies of the decays $D^0 \rightarrow K_S^0K^-\pi^+$ and $D^0 \rightarrow K_S^0K^+\pi^-$* , *Phys. Rev. D* **85** (2012) 092016 [Erratum *ibid.* **94** (2016) 099905] [[arXiv:1203.3804](#)] [[INSPIRE](#)].
- [51] LHCb collaboration, *Studies of the resonance structure in $D^0 \rightarrow K_S^0K^\pm\pi^\mp$ decays*, *Phys. Rev. D* **93** (2016) 052018 [[arXiv:1509.06628](#)] [[INSPIRE](#)].
- [52] M. Bjørn and S. Malde, *CP violation and material interaction of neutral kaons in measurements of the CKM angle γ using $B^\pm \rightarrow DK^\pm$ decays where $D \rightarrow K_S^0\pi^+\pi^-$* , *JHEP* **07** (2019) 106 [[arXiv:1904.01129](#)] [[INSPIRE](#)].

- [53] CLEO collaboration, *Model-independent determination of the strong-phase difference between D^0 and $\bar{D}^0 \rightarrow K_{S,L}^0 h^+ h^-$ ($h = \pi, K$) and its impact on the measurement of the CKM angle γ/ϕ_3* , *Phys. Rev. D* **82** (2010) 112006 [[arXiv:1010.2817](#)] [[INSPIRE](#)].
- [54] BESIII collaboration, *Model-independent determination of the relative strong-phase difference between D^0 and $\bar{D}^0 \rightarrow K_{S,L}^0 \pi^+ \pi^-$ and its impact on the measurement of the CKM angle γ/ϕ_3* , *Phys. Rev. D* **101** (2020) 112002 [[arXiv:2003.00091](#)] [[INSPIRE](#)].
- [55] BESIII collaboration, *Determination of strong-phase parameters in $D \rightarrow K_{S,L}^0 \pi^+ \pi^-$* , *Phys. Rev. Lett.* **124** (2020) 241802 [[arXiv:2002.12791](#)] [[INSPIRE](#)].
- [56] BESIII collaboration, *Improved model-independent determination of the strong-phase difference between D^0 and $\bar{D}^0 \rightarrow K_{S,L}^0 K^+ K^-$ decays*, *Phys. Rev. D* **102** (2020) 052008 [[arXiv:2007.07959](#)] [[INSPIRE](#)].
- [57] B. Sen, M. Walker and M. Woodroffe, *On the unified method with nuisance parameters*, *Statist. Sinica* **19** (2009) 301.
- [58] CLEO collaboration, *Updated measurement of the strong phase in $D^0 \rightarrow K^+ \pi^-$ decay using quantum correlations in $e^+ e^- \rightarrow D^0 \bar{D}^0$ at CLEO*, *Phys. Rev. D* **86** (2012) 112001 [[arXiv:1210.0939](#)] [[INSPIRE](#)].
- [59] BESIII collaboration, *Measurement of the $D \rightarrow K^- \pi^+$ strong phase difference in $\psi(3770) \rightarrow D^0 \bar{D}^0$* , *Phys. Lett. B* **734** (2014) 227 [[arXiv:1404.4691](#)] [[INSPIRE](#)].
- [60] T. Pajero and M.J. Morello, *Mixing and CP violation in $D^0 \rightarrow K^- \pi^+$ decays*, [arXiv:2106.02014](#) [[INSPIRE](#)].

The LHCb collaboration

R. Aaij³², A.S.W. Abdelmotteb⁵⁶, C. Abellán Beteta⁵⁰, F. Abudinén⁵⁶, T. Ackernley⁶⁰, B. Adeva⁴⁶, M. Adinolfi⁵⁴, H. Afsharnia⁹, C. Agapopoulou¹³, C.A. Aidala⁸⁷, S. Aiola²⁵, Z. Ajaltouni⁹, S. Akar⁶⁵, J. Albrecht¹⁵, F. Alessio⁴⁸, M. Alexander⁵⁹, A. Alfonso Albero⁴⁵, Z. Aliouche⁶², G. Alkhazov³⁸, P. Alvarez Cartelle⁵⁵, S. Amato², J.L. Amey⁵⁴, Y. Amhis¹¹, L. An⁴⁸, L. Anderlini²², A. Andreianov³⁸, M. Andreotti²¹, F. Archilli¹⁷, A. Artamonov⁴⁴, M. Artuso⁶⁸, K. Arzymatov⁴², E. Aslanides¹⁰, M. Atzeni⁵⁰, B. Audurier¹², S. Bachmann¹⁷, M. Bachmayer⁴⁹, J.J. Back⁵⁶, P. Baladron Rodriguez⁴⁶, V. Balagura¹², W. Baldini²¹, J. Baptista Leite¹, M. Barbetti^{22,g}, R.J. Barlow⁶², S. Barsuk¹¹, W. Barter⁶¹, M. Bartolini^{24,h}, F. Baryshnikov⁸³, J.M. Basels¹⁴, S. Bashir³⁴, G. Bassi²⁹, B. Batsukh⁶⁸, A. Battig¹⁵, A. Bay⁴⁹, A. Beck⁵⁶, M. Becker¹⁵, F. Bedeschi²⁹, I. Bediaga¹, A. Beiter⁶⁸, V. Belavin⁴², S. Belin²⁷, V. Bellee⁵⁰, K. Belous⁴⁴, I. Belov⁴⁰, I. Belyaev⁴¹, G. Bencivenni²³, E. Ben-Haim¹³, A. Berezhnoy⁴⁰, R. Bernet⁵⁰, D. Berninghoff¹⁷, H.C. Bernstein⁶⁸, C. Bertella⁴⁸, A. Bertolin²⁸, C. Betancourt⁵⁰, F. Betti⁴⁸, Ia. Bezshyiko⁵⁰, S. Bhasin⁵⁴, J. Bhom³⁵, L. Bian⁷³, M.S. Bieker¹⁵, S. Bifani⁵³, P. Billoir¹³, M. Birch⁶¹, F.C.R. Bishop⁵⁵, A. Bitadze⁶², A. Bizzeti^{22,k}, M. Bjørn⁶³, M.P. Blago⁴⁸, T. Blake⁵⁶, F. Blanc⁴⁹, S. Blusk⁶⁸, D. Bobulska⁵⁹, J.A. Boelhauve¹⁵, O. Boente Garcia⁴⁶, T. Boettcher⁶⁵, A. Boldyrev⁸², A. Bondar⁴³, N. Bondar^{38,48}, S. Borghi⁶², M. Borisyak⁴², M. Borsato¹⁷, J.T. Borsuk³⁵, S.A. Bouchiba⁴⁹, T.J.V. Bowcock⁶⁰, A. Boyer⁴⁸, C. Bozzi²¹, M.J. Bradley⁶¹, S. Braun⁶⁶, A. Brea Rodriguez⁴⁶, J. Brodzicka³⁵, A. Brossa Gonzalo⁵⁶, D. Brundu²⁷, A. Buonauro⁵⁰, L. Buonincontri²⁸, A.T. Burke⁶², C. Burr⁴⁸, A. Bursche⁷², A. Butkevich³⁹, J.S. Butter³², J. Buytaert⁴⁸, W. Byczynski⁴⁸, S. Cadeddu²⁷, H. Cai⁷³, R. Calabrese^{21,f}, L. Calefice^{15,13}, L. Calero Diaz²³, S. Cali²³, R. Calladine⁵³, M. Calvi^{26,j}, M. Calvo Gomez⁸⁵, P. Camargo Magalhaes⁵⁴, P. Campana²³, A.F. Campoverde Quezada⁶, S. Capelli^{26,j}, L. Capriotti^{20,d}, A. Carbone^{20,d}, G. Carboni³¹, R. Cardinale^{24,h}, A. Cardini²⁷, I. Carli⁴, P. Carniti^{26,j}, L. Carus¹⁴, K. Carvalho Akiba³², A. Casais Vidal⁴⁶, G. Casse⁶⁰, M. Cattaneo⁴⁸, G. Cavallero⁴⁸, S. Celani⁴⁹, J. Cerasoli¹⁰, D. Cervenkov⁶³, A.J. Chadwick⁶⁰, M.G. Chapman⁵⁴, M. Charles¹³, Ph. Charpentier⁴⁸, G. Chatzikonstantinidis⁵³, C.A. Chavez Barajas⁶⁰, M. Chefdeville⁸, C. Chen³, S. Chen⁴, A. Chernov³⁵, V. Chobanova⁴⁶, S. Cholak⁴⁹, M. Chruszcz³⁵, A. Chubykin³⁸, V. Chulikov³⁸, P. Ciambrone²³, M.F. Cicala⁵⁶, X. Cid Vidal⁴⁶, G. Ciezarek⁴⁸, P.E.L. Clarke⁵⁸, M. Clemencic⁴⁸, H.V. Cliff⁵⁵, J. Closier⁴⁸, J.L. Cobbedick⁶², V. Coco⁴⁸, J.A.B. Coelho¹¹, J. Cogan¹⁰, E. Cogneras⁹, L. Cojocariu³⁷, P. Collins⁴⁸, T. Colombo⁴⁸, L. Congedo^{19,c}, A. Contu²⁷, N. Cooke⁵³, G. Coombs⁵⁹, I. Corredoira⁴⁶, G. Corti⁴⁸, C.M. Costa Sobral⁵⁶, B. Couturier⁴⁸, D.C. Craik⁶⁴, J. Crkovská⁶⁷, M. Cruz Torres¹, R. Currie⁵⁸, C.L. Da Silva⁶⁷, S. Dadabaev⁸³, L. Dai⁷¹, E. Dall'Occo¹⁵, J. Dalseno⁴⁶, C. D'Ambrosio⁴⁸, A. Danilina⁴¹, P. d'Argent⁴⁸, J.E. Davies⁶², A. Davis⁶², O. De Aguiar Francisco⁶², K. De Bruyn⁷⁹, S. De Capua⁶², M. De Cian⁴⁹, J.M. De Miranda¹, L. De Paula², M. De Serio^{19,c}, D. De Simone⁵⁰, P. De Simone²³, F. De Vellis¹⁵, J.A. de Vries⁸⁰, C.T. Dean⁶⁷, F. Debernardis^{19,c}, D. Decamp⁸, V. Dedu¹⁰, L. Del Buono¹³, B. Delaney⁵⁵, H.-P. Dembinski¹⁵, A. Dendek³⁴, V. Denysenko⁵⁰, D. Derkach⁸², O. Deschamps⁹, F. Desse¹¹, F. Dettori^{27,e}, B. Dey⁷⁷, A. Di Cicco²³, P. Di Nezza²³, S. Didenko⁸³, L. Dieste Maronas⁴⁶, H. Dijkstra⁴⁸, V. Dobishuk⁵², C. Dong³, A.M. Donohoe¹⁸, F. Dordei²⁷, A.C. dos Reis¹, L. Douglas⁵⁹, A. Dovbnya⁵¹, A.G. Downes⁸, M.W. Dudek³⁵, L. Dufour⁴⁸, V. Duk⁷⁸, P. Durante⁴⁸, J.M. Durham⁶⁷, D. Dutta⁶², A. Dziurda³⁵, A. Dzyuba³⁸, S. Easo⁵⁷, U. Egede⁶⁹, V. Egorychev⁴¹, S. Eidelman^{43,u,†}, S. Eisenhardt⁵⁸, S. Ek-In⁴⁹, L. Eklund^{59,86}, S. Ely⁶⁸, A. Ene³⁷, E. Eppele⁶⁷, S. Escher¹⁴, J. Eschle⁵⁰, S. Esen¹³, T. Evans⁴⁸, A. Falabella²⁰, J. Fan³, Y. Fan⁶, B. Fang⁷³, S. Farry⁶⁰, D. Fazzini^{26,j}, M. Féo⁴⁸, A. Fernandez Prieto⁴⁶, A.D. Fernez⁶⁶, F. Ferrari^{20,d}, L. Ferreira Lopes⁴⁹, F. Ferreira Rodrigues²,

S. Ferreres Sole³², M. Ferrillo⁵⁰, M. Ferro-Luzzi⁴⁸, S. Filippov³⁹, R.A. Fini¹⁹, M. Fiorini^{21,f}, M. Firlej³⁴, K.M. Fischer⁶³, D.S. Fitzgerald⁸⁷, C. Fitzpatrick⁶², T. Fiutowski³⁴, A. Fkias⁴⁸, F. Fleuret¹², M. Fontana¹³, F. Fontanelli^{24,h}, R. Forty⁴⁸, D. Foulds-Holt⁵⁵, V. Franco Lima⁶⁰, M. Franco Sevilla⁶⁶, M. Frank⁴⁸, E. Franzoso²¹, G. Frau¹⁷, C. Frei⁴⁸, D.A. Friday⁵⁹, J. Fu⁶, Q. Fuehring¹⁵, E. Gabriel³², G. Galati^{19,c}, A. Gallas Torreira⁴⁶, D. Galli^{20,d}, S. Gambetta^{58,48}, Y. Gan³, M. Gandelman², P. Gandini²⁵, Y. Gao⁵, M. Garau²⁷, L.M. Garcia Martin⁵⁶, P. Garcia Moreno⁴⁵, J. García Pardiñas^{26,j}, B. Garcia Plana⁴⁶, F.A. Garcia Rosales¹², L. Garrido⁴⁵, C. Gaspar⁴⁸, R.E. Geertsema³², D. Gerick¹⁷, L.L. Gerken¹⁵, E. Gersabeck⁶², M. Gersabeck⁶², T. Gershon⁵⁶, D. Gerstel¹⁰, L. Giambastiani²⁸, V. Gibson⁵⁵, H.K. Giemza³⁶, A.L. Gilman⁶³, M. Giovannetti^{23,p}, A. Gioventù⁴⁶, P. Gironella Gironell⁴⁵, L. Giubega³⁷, C. Giugliano^{21,f,48}, K. Gizdov⁵⁸, E.L. Gkougkousis⁴⁸, V.V. Gligorov¹³, C. Göbel⁷⁰, E. Golobardes⁸⁵, D. Golubkov⁴¹, A. Golutvin^{61,83}, A. Gomes^{1,a}, S. Gomez Fernandez⁴⁵, F. Goncalves Abrantes⁶³, M. Goncerz³⁵, G. Gong³, P. Gorbounov⁴¹, I.V. Gorelov⁴⁰, C. Gotti²⁶, E. Govorkova⁴⁸, J.P. Grabowski¹⁷, T. Grammatico¹³, L.A. Granado Cardoso⁴⁸, E. Graugés⁴⁵, E. Graverini⁴⁹, G. Graziani²², A. Grecu³⁷, L.M. Greeven³², N.A. Grieser⁴, L. Grillo⁶², S. Gromov⁸³, B.R. Gruberg Cazon⁶³, C. Gu³, M. Guarise²¹, M. Guittiere¹¹, P. A. Günther¹⁷, E. Gushchin³⁹, A. Guth¹⁴, Y. Guz⁴⁴, T. Gys⁴⁸, T. Hadavizadeh⁶⁹, G. Haefeli⁴⁹, C. Haen⁴⁸, J. Haimberger⁴⁸, T. Halewood-leagas⁶⁰, P.M. Hamilton⁶⁶, J.P. Hammerich⁶⁰, Q. Han⁷, X. Han¹⁷, T.H. Hancock⁶³, E.B. Hansen⁶², S. Hansmann-Menzemer¹⁷, N. Harnew⁶³, T. Harrison⁶⁰, C. Hasse⁴⁸, M. Hatch⁴⁸, J. He^{6,b}, M. Hecker⁶¹, K. Heijhoff³², K. Heinicke¹⁵, A.M. Hennequin⁴⁸, K. Hennessy⁶⁰, L. Henry⁴⁸, J. Heuel¹⁴, A. Hicheur², D. Hill⁴⁹, M. Hilton⁶², S.E. Hollitt¹⁵, R. Hou⁷, Y. Hou⁸, J. Hu¹⁷, J. Hu⁷², W. Hu⁷, X. Hu³, W. Huang⁶, X. Huang⁷³, W. Hulsbergen³², R.J. Hunter⁵⁶, M. Hushchyn⁸², D. Hutchcroft⁶⁰, D. Hynds³², P. Ibis¹⁵, M. Idzik³⁴, D. Ilin³⁸, P. Ilten⁶⁵, A. Inglessi³⁸, A. Ishteev⁸³, K. Ivshin³⁸, R. Jacobsson⁴⁸, H. Jage¹⁴, S. Jakobsen⁴⁸, E. Jans³², B.K. Jashal⁴⁷, A. Jawahery⁶⁶, V. Jevtic¹⁵, F. Jiang³, M. John⁶³, D. Johnson⁴⁸, C.R. Jones⁵⁵, T.P. Jones⁵⁶, B. Jost⁴⁸, N. Jurik⁴⁸, S.H. Kalavan Kadavath³⁴, S. Kandybei⁵¹, Y. Kang³, M. Karacson⁴⁸, M. Karpov⁸², F. Keizer⁴⁸, D.M. Keller⁶⁸, M. Kenzie⁵⁶, T. Ketel³³, B. Khanji¹⁵, A. Kharisova⁸⁴, S. Kholodenko⁴⁴, T. Kirn¹⁴, V.S. Kirsebom⁴⁹, O. Kitouni⁶⁴, S. Klaver³², N. Kleijne²⁹, K. Klimaszewski³⁶, M.R. Kmiec³⁶, S. Koliiev⁵², A. Kondybayeva⁸³, A. Konoplyannikov⁴¹, P. Kopciwicz³⁴, R. Kopečna¹⁷, P. Koppenburg³², M. Korolev⁴⁰, I. Kostiuik^{32,52}, O. Kot⁵², S. Kotriakhova^{21,38}, P. Kravchenko³⁸, L. Kravchuk³⁹, R.D. Krawczyk⁴⁸, M. Kreps⁵⁶, F. Kress⁶¹, S. Kretzschmar¹⁴, P. Krokovny^{43,u}, W. Krupa³⁴, W. Krzemien³⁶, M. Kucharczyk³⁵, V. Kudryavtsev^{43,u}, H.S. Kuindersma^{32,33}, G.J. Kunde⁶⁷, T. Kvaratskheliya⁴¹, D. Lacarrere⁴⁸, G. Lafferty⁶², A. Lai²⁷, A. Lampis²⁷, D. Lancierini⁵⁰, J.J. Lane⁶², R. Lane⁵⁴, G. Lanfranchi²³, C. Langenbruch¹⁴, J. Langer¹⁵, O. Lantwin⁸³, T. Latham⁵⁶, F. Lazzari^{29,q}, R. Le Gac¹⁰, S.H. Lee⁸⁷, R. Lefèvre⁹, A. Leflat⁴⁰, S. Legotin⁸³, O. Leroy¹⁰, T. Lesiak³⁵, B. Leverington¹⁷, H. Li⁷², P. Li¹⁷, S. Li⁷, Y. Li⁴, Y. Li⁴, Z. Li⁶⁸, X. Liang⁶⁸, T. Lin⁶¹, R. Lindner⁴⁸, V. Lisovskyi¹⁵, R. Litvinov²⁷, G. Liu⁷², H. Liu⁶, Q. Liu⁶, S. Liu⁴, A. Lobo Salvia⁴⁵, A. Loi²⁷, J. Lomba Castro⁴⁶, I. Longstaff⁵⁹, J.H. Lopes², S. Lopez Solino⁴⁶, G.H. Lovell⁵⁵, Y. Lu⁴, C. Lucarelli^{22,g}, D. Lucchesi^{28,l}, S. Luchuk³⁹, M. Lucio Martinez³², V. Lukashenko^{32,52}, Y. Luo³, A. Lupato⁶², E. Luppi^{21,f}, O. Lupton⁵⁶, A. Lusiani^{29,m}, X. Lyu⁶, L. Ma⁴, R. Ma⁶, S. Maccolini^{20,d}, F. Machefert¹¹, F. Maciuc³⁷, V. Macko⁴⁹, P. Mackowiak¹⁵, S. Maddrell-Mander⁵⁴, O. Madejczyk³⁴, L.R. Madhan Mohan⁵⁴, O. Maev³⁸, A. Maevskiy⁸², D. Maisuzenko³⁸, M.W. Majewski³⁴, J.J. Malczewski³⁵, S. Malde⁶³, B. Malecki⁴⁸, A. Malinin⁸¹, T. Maltsev^{43,u}, H. Malygina¹⁷, G. Manca^{27,e}, G. Mancinelli¹⁰, D. Manuzzi^{20,d}, D. Marangotto^{25,i}, J. Maratas^{9,s}, J.F. Marchand⁸, U. Marconi²⁰, S. Mariani^{22,g}, C. Marin Benito⁴⁸, M. Marinangeli⁴⁹, J. Marks¹⁷, A.M. Marshall⁵⁴, P.J. Marshall⁶⁰, G. Martelli⁷⁸, G. Martellotti³⁰, L. Martinazzoli^{48,j}, M. Martinelli^{26,j}, D. Martinez Santos⁴⁶, F. Martinez Vidal⁴⁷, A. Massafferri¹,

M. Materok¹⁴, R. Matev⁴⁸, A. Mathad⁵⁰, V. Matiunin⁴¹, C. Matteuzzi²⁶, K.R. Mattioli⁸⁷, A. Mauri³², E. Maurice¹², J. Mauricio⁴⁵, M. Mazurek⁴⁸, M. McCann⁶¹, L. McConnell¹⁸, T.H. Mcgrath⁶², N.T. Mchugh⁵⁹, A. McNab⁶², R. McNulty¹⁸, J.V. Mead⁶⁰, B. Meadows⁶⁵, G. Meier¹⁵, N. Meinert⁷⁶, D. Melnychuk³⁶, S. Meloni^{26,j}, M. Merk^{32,80}, A. Merli^{25,i}, L. Meyer Garcia², M. Mikhasenko⁴⁸, D.A. Milanes⁷⁴, E. Millard⁵⁶, M. Milovanovic⁴⁸, M.-N. Minard⁸, A. Minotti^{26,j}, L. Minzoni^{21,f}, S.E. Mitchell⁵⁸, B. Mitreska⁶², D.S. Mitzel¹⁵, A. Mödden¹⁵, R.A. Mohammed⁶³, R.D. Moise⁶¹, S. Mokhnenko⁸², T. Mombächer⁴⁶, I.A. Monroy⁷⁴, S. Monteil⁹, M. Morandin²⁸, G. Morello²³, M.J. Morello^{29,m}, J. Moron³⁴, A.B. Morris⁷⁵, A.G. Morris⁵⁶, R. Mountain⁶⁸, H. Mu³, F. Muheim^{58,48}, M. Mulder⁴⁸, D. Müller⁴⁸, K. Müller⁵⁰, C.H. Murphy⁶³, D. Murray⁶², P. Muzzetto^{27,48}, P. Naik⁵⁴, T. Nakada⁴⁹, R. Nandakumar⁵⁷, T. Nanut⁴⁹, I. Nasteva², M. Needham⁵⁸, I. Neri²¹, N. Neri^{25,i}, S. Neubert⁷⁵, N. Neufeld⁴⁸, R. Newcombe⁶¹, E.M. Niel¹¹, S. Nieswand¹⁴, N. Nikitin⁴⁰, N.S. Nolte⁶⁴, C. Normand⁸, C. Nunez⁸⁷, A. Oblakowska-Mucha³⁴, V. Obraztsov⁴⁴, T. Oeser¹⁴, D.P. O’Hanlon⁵⁴, S. Okamura²¹, R. Oldeman^{27,e}, F. Oliva⁵⁸, M.E. Olivares⁶⁸, C.J.G. Onderwater⁷⁹, R.H. O’Neil⁵⁸, J.M. Otalora Goicochea², T. Ovsianikova⁴¹, P. Owen⁵⁰, A. Oyanguren⁴⁷, K.O. Padeken⁷⁵, B. Pagare⁵⁶, P.R. Pais⁴⁸, T. Pajero⁶³, A. Palano¹⁹, M. Palutan²³, Y. Pan⁶², G. Panshin⁸⁴, A. Papanestis⁵⁷, M. Pappagallo^{19,c}, L.L. Pappalardo^{21,f}, C. Pappenheimer⁶⁵, W. Parker⁶⁶, C. Parkes⁶², B. Passalacqua²¹, G. Passaleva²², A. Pastore¹⁹, M. Patel⁶¹, C. Patrignani^{20,d}, C.J. Pawley⁸⁰, A. Pearce⁴⁸, A. Pellegrino³², M. Pepe Altarelli⁴⁸, S. Perazzini²⁰, D. Pereima⁴¹, A. Pereiro Castro⁴⁶, P. Perret⁹, M. Petric^{59,48}, K. Petridis⁵⁴, A. Petrolini^{24,h}, A. Petrov⁸¹, S. Petrucci⁵⁸, M. Petruzzo²⁵, T.T.H. Pham⁶⁸, A. Philippov⁴², L. Pica^{29,m}, M. Piccini⁷⁸, B. Pietrzyk⁸, G. Pietrzyk⁴⁹, M. Pili⁶³, D. Pinci³⁰, F. Pisani⁴⁸, M. Pizzichemi^{26,48,j}, Resmi P.K¹⁰, V. Placinta³⁷, J. Plews⁵³, M. Plo Casasus⁴⁶, F. Polci¹³, M. Poli Lener²³, M. Poliakova⁶⁸, A. Poluektov¹⁰, N. Polukhina^{83,t}, I. Polyakov⁶⁸, E. Polycarpo², S. Ponce⁴⁸, D. Popov^{6,48}, S. Popov⁴², S. Poslavskii⁴⁴, K. Prasanthi³⁵, L. Promberger⁴⁸, C. Prouve⁴⁶, V. Pugatch⁵², V. Puill¹¹, H. Pullen⁶³, G. Punzi^{29,n}, H. Qi³, W. Qian⁶, J. Qin⁶, N. Qin³, R. Quagliani⁴⁹, B. Quintana⁸, N.V. Raab¹⁸, R.I. Rabadan Trejo⁶, B. Rachwal³⁴, J.H. Rademacker⁵⁴, M. Rama²⁹, M. Ramos Pernas⁵⁶, M.S. Rangel², F. Ratnikov^{42,82}, G. Raven³³, M. Reboud⁸, F. Redi⁴⁹, F. Reiss⁶², C. Remon Alepez⁴⁷, Z. Ren³, V. Renaudin⁶³, R. Ribatti²⁹, S. Ricciardi⁵⁷, K. Rinnert⁶⁰, P. Robbe¹¹, G. Robertson⁵⁸, A.B. Rodrigues⁴⁹, E. Rodrigues⁶⁰, J.A. Rodriguez Lopez⁷⁴, E.R.R. Rodriguez Rodriguez⁴⁶, A. Rollings⁶³, P. Roloff⁴⁸, V. Romanovskiy⁴⁴, M. Romero Lamas⁴⁶, A. Romero Vidal⁴⁶, J.D. Roth⁸⁷, M. Rotondo²³, M.S. Rudolph⁶⁸, T. Ruf⁴⁸, R.A. Ruiz Fernandez⁴⁶, J. Ruiz Vidal⁴⁷, A. Ryzhikov⁸², J. Ryzka³⁴, J.J. Saborido Silva⁴⁶, N. Sagidova³⁸, N. Sahoo⁵⁶, B. Saitta^{27,e}, M. Salomoni⁴⁸, C. Sanchez Gras³², R. Santacesaria³⁰, C. Santamarina Rios⁴⁶, M. Santimaria²³, E. Santovetti^{31,p}, D. Saranin⁸³, G. Sarpis¹⁴, M. Sarpis⁷⁵, A. Sarti³⁰, C. Satriano^{30,o}, A. Satta³¹, M. Saur¹⁵, D. Savrina^{41,40}, H. Sazak⁹, L.G. Scantlebury Smead⁶³, A. Scarabotto¹³, S. Schael¹⁴, S. Scherl⁶⁰, M. Schiller⁵⁹, H. Schindler⁴⁸, M. Schmelling¹⁶, B. Schmidt⁴⁸, S. Schmitt¹⁴, O. Schneider⁴⁹, A. Schopper⁴⁸, M. Schubiger³², S. Schulte⁴⁹, M.H. Schune¹¹, R. Schwemmer⁴⁸, B. Sciascia^{23,48}, S. Sellam⁴⁶, A. Semennikov⁴¹, M. Senghi Soares³³, A. Sergi^{24,h}, N. Serra⁵⁰, L. Sestini²⁸, A. Seuthe¹⁵, Y. Shang⁵, D.M. Shangase⁸⁷, M. Shapkin⁴⁴, I. Shchemerov⁸³, L. Shchutska⁴⁹, T. Shears⁶⁰, L. Shekhtman^{43,u}, Z. Shen⁵, V. Shevchenko⁸¹, E.B. Shields^{26,j}, Y. Shimizu¹¹, E. Shmanin⁸³, J.D. Shupperd⁶⁸, B.G. Siddi²¹, R. Silva Coutinho⁵⁰, G. Simi²⁸, S. Simone^{19,c}, N. Skidmore⁶², T. Skwarnicki⁶⁸, M.W. Slater⁵³, I. Slazyk^{21,f}, J.C. Smallwood⁶³, J.G. Smeaton⁵⁵, A. Smetkina⁴¹, E. Smith⁵⁰, M. Smith⁶¹, A. Snoch³², M. Soares²⁰, L. Soares Lavra⁹, M.D. Sokoloff⁶⁵, F.J.P. Soler⁵⁹, A. Solovev³⁸, I. Solovyev³⁸, F.L. Souza De Almeida², B. Souza De Paula², B. Spaan¹⁵, E. Spadaro Norella^{25,i}, P. Spradlin⁵⁹, F. Stagni⁴⁸, M. Stahl⁶⁵, S. Stahl⁴⁸, S. Stanislaus⁶³, O. Steinkamp^{50,83}, O. Stenyakin⁴⁴, H. Stevens¹⁵, S. Stone⁶⁸, M. Straticiu³⁷,

D. Strelakina⁸³, F. Suljik⁶³, J. Sun²⁷, L. Sun⁷³, Y. Sun⁶⁶, P. Svihra⁶², P.N. Swallow⁵³, K. Swientek³⁴, A. Szabelski³⁶, T. Szumlak³⁴, M. Szymanski⁴⁸, S. Taneja⁶², A.R. Tanner⁵⁴, M.D. Tat⁶³, A. Terentev⁸³, F. Teubert⁴⁸, E. Thomas⁴⁸, D.J.D. Thompson⁵³, K.A. Thomson⁶⁰, V. Tisserand⁹, S. T'Jampens⁸, M. Tobin⁴, L. Tomassetti^{21,f}, X. Tong⁵, D. Torres Machado¹, D.Y. Tou¹³, E. Trifonova⁸³, C. Tripl⁴⁹, G. Tuci⁶, A. Tully⁴⁹, N. Tuning^{32,48}, A. Ukleja³⁶, D.J. Unverzagt¹⁷, E. Ursov⁸³, A. Usachov³², A. Ustyuzhanin^{42,82}, U. Uwer¹⁷, A. Vagner⁸⁴, V. Vagnoni²⁰, A. Valassi⁴⁸, G. Valenti²⁰, N. Valls Canudas⁸⁵, M. van Beuzekom³², M. Van Dijk⁴⁹, H. Van Hecke⁶⁷, E. van Herwijnen⁸³, C.B. Van Hulse¹⁸, M. van Veghel⁷⁹, R. Vazquez Gomez⁴⁵, P. Vazquez Regueiro⁴⁶, C. Vázquez Sierra⁴⁸, S. Vecchi²¹, J.J. Velthuis⁵⁴, M. Veltri^{22,r}, A. Venkateswaran⁶⁸, M. Veronesi³², M. Vesterinen⁵⁶, D. Vieira⁶⁵, M. Vieites Diaz⁴⁹, H. Viemann⁷⁶, X. Vilasis-Cardona⁸⁵, E. Vilella Figueras⁶⁰, A. Villa²⁰, P. Vincent¹³, F.C. Volle¹¹, D. Vom Bruch¹⁰, A. Vorobyev³⁸, V. Vorobyev^{43,u}, N. Voropaev³⁸, K. Vos⁸⁰, R. Waldi¹⁷, J. Walsh²⁹, C. Wang¹⁷, J. Wang⁵, J. Wang⁴, J. Wang³, J. Wang⁷³, M. Wang³, R. Wang⁵⁴, Y. Wang⁷, Z. Wang⁵⁰, Z. Wang³, Z. Wang⁶, J.A. Ward⁵⁶, N.K. Watson⁵³, S.G. Weber¹³, D. Websdale⁶¹, C. Weisser⁶⁴, B.D.C. Westhenry⁵⁴, D.J. White⁶², M. Whitehead⁵⁴, A.R. Wiederhold⁵⁶, D. Wiedner¹⁵, G. Wilkinson⁶³, M. Wilkinson⁶⁸, I. Williams⁵⁵, M. Williams⁶⁴, M.R.J. Williams⁵⁸, F.F. Wilson⁵⁷, W. Wislicki³⁶, M. Witek³⁵, L. Witola¹⁷, G. Wormser¹¹, S.A. Wotton⁵⁵, H. Wu⁶⁸, K. Wyllie⁴⁸, Z. Xiang⁶, D. Xiao⁷, Y. Xie⁷, A. Xu⁵, J. Xu⁶, L. Xu³, M. Xu⁷, Q. Xu⁶, Z. Xu⁵, Z. Xu⁶, D. Yang³, S. Yang⁶, Y. Yang⁶, Z. Yang⁵, Z. Yang⁶⁶, Y. Yao⁶⁸, L.E. Yeomans⁶⁰, H. Yin⁷, J. Yu⁷¹, X. Yuan⁶⁸, O. Yushchenko⁴⁴, E. Zaffaroni⁴⁹, M. Zavertyaev^{16,t}, M. Zdybal³⁵, O. Zenaiev⁴⁸, M. Zeng³, D. Zhang⁷, L. Zhang³, S. Zhang⁷¹, S. Zhang⁵, Y. Zhang⁵, Y. Zhang⁶³, A. Zharkova⁸³, A. Zhelezov¹⁷, Y. Zheng⁶, T. Zhou⁵, X. Zhou⁶, Y. Zhou⁶, V. Zhovkovska¹¹, X. Zhu³, X. Zhu⁷, Z. Zhu⁶, V. Zhukov^{14,40}, J.B. Zonneveld⁵⁸, Q. Zou⁴, S. Zucchelli^{20,d}, D. Zuliani²⁸ and G. Zunica⁶²

¹ Centro Brasileiro de Pesquisas Físicas (CBPF), Rio de Janeiro, Brazil

² Universidade Federal do Rio de Janeiro (UFRJ), Rio de Janeiro, Brazil

³ Center for High Energy Physics, Tsinghua University, Beijing, China

⁴ Institute Of High Energy Physics (IHEP), Beijing, China

⁵ School of Physics State Key Laboratory of Nuclear Physics and Technology, Peking University, Beijing, China

⁶ University of Chinese Academy of Sciences, Beijing, China

⁷ Institute of Particle Physics, Central China Normal University, Wuhan, Hubei, China

⁸ Univ. Savoie Mont Blanc, CNRS, IN2P3-LAPP, Annecy, France

⁹ Université Clermont Auvergne, CNRS/IN2P3, LPC, Clermont-Ferrand, France

¹⁰ Aix Marseille Univ, CNRS/IN2P3, CPPM, Marseille, France

¹¹ Université Paris-Saclay, CNRS/IN2P3, IJCLab, Orsay, France

¹² Laboratoire Leprince-Ringuet, CNRS/IN2P3, Ecole Polytechnique, Institut Polytechnique de Paris, Palaiseau, France

¹³ LPNHE, Sorbonne Université, Paris Diderot Sorbonne Paris Cité, CNRS/IN2P3, Paris, France

¹⁴ I. Physikalisches Institut, RWTH Aachen University, Aachen, Germany

¹⁵ Fakultät Physik, Technische Universität Dortmund, Dortmund, Germany

¹⁶ Max-Planck-Institut für Kernphysik (MPIK), Heidelberg, Germany

¹⁷ Physikalisches Institut, Ruprecht-Karls-Universität Heidelberg, Heidelberg, Germany

¹⁸ School of Physics, University College Dublin, Dublin, Ireland

¹⁹ INFN Sezione di Bari, Bari, Italy

²⁰ INFN Sezione di Bologna, Bologna, Italy

²¹ INFN Sezione di Ferrara, Ferrara, Italy

²² INFN Sezione di Firenze, Firenze, Italy

²³ INFN Laboratori Nazionali di Frascati, Frascati, Italy

- 24 *INFN Sezione di Genova, Genova, Italy*
- 25 *INFN Sezione di Milano, Milano, Italy*
- 26 *INFN Sezione di Milano-Bicocca, Milano, Italy*
- 27 *INFN Sezione di Cagliari, Monserrato, Italy*
- 28 *Universita degli Studi di Padova, Universita e INFN, Padova, Padova, Italy*
- 29 *INFN Sezione di Pisa, Pisa, Italy*
- 30 *INFN Sezione di Roma La Sapienza, Roma, Italy*
- 31 *INFN Sezione di Roma Tor Vergata, Roma, Italy*
- 32 *Nikhef National Institute for Subatomic Physics, Amsterdam, Netherlands*
- 33 *Nikhef National Institute for Subatomic Physics and VU University Amsterdam, Amsterdam, Netherlands*
- 34 *AGH — University of Science and Technology, Faculty of Physics and Applied Computer Science, Kraków, Poland*
- 35 *Henryk Niewodniczanski Institute of Nuclear Physics Polish Academy of Sciences, Kraków, Poland*
- 36 *National Center for Nuclear Research (NCBJ), Warsaw, Poland*
- 37 *Horia Hulubei National Institute of Physics and Nuclear Engineering, Bucharest-Magurele, Romania*
- 38 *Petersburg Nuclear Physics Institute NRC Kurchatov Institute (PNPI NRC KI), Gatchina, Russia*
- 39 *Institute for Nuclear Research of the Russian Academy of Sciences (INR RAS), Moscow, Russia*
- 40 *Institute of Nuclear Physics, Moscow State University (SINP MSU), Moscow, Russia*
- 41 *Institute of Theoretical and Experimental Physics NRC Kurchatov Institute (ITEP NRC KI), Moscow, Russia*
- 42 *Yandex School of Data Analysis, Moscow, Russia*
- 43 *Budker Institute of Nuclear Physics (SB RAS), Novosibirsk, Russia*
- 44 *Institute for High Energy Physics NRC Kurchatov Institute (IHEP NRC KI), Protvino, Russia, Protvino, Russia*
- 45 *ICCUB, Universitat de Barcelona, Barcelona, Spain*
- 46 *Instituto Galego de Física de Altas Enerxías (IGFAE), Universidade de Santiago de Compostela, Santiago de Compostela, Spain*
- 47 *Instituto de Física Corpuscular, Centro Mixto Universidad de Valencia — CSIC, Valencia, Spain*
- 48 *European Organization for Nuclear Research (CERN), Geneva, Switzerland*
- 49 *Institute of Physics, Ecole Polytechnique Fédérale de Lausanne (EPFL), Lausanne, Switzerland*
- 50 *Physik-Institut, Universität Zürich, Zürich, Switzerland*
- 51 *NSC Kharkiv Institute of Physics and Technology (NSC KIPT), Kharkiv, Ukraine*
- 52 *Institute for Nuclear Research of the National Academy of Sciences (KINR), Kyiv, Ukraine*
- 53 *University of Birmingham, Birmingham, United Kingdom*
- 54 *H.H. Wills Physics Laboratory, University of Bristol, Bristol, United Kingdom*
- 55 *Cavendish Laboratory, University of Cambridge, Cambridge, United Kingdom*
- 56 *Department of Physics, University of Warwick, Coventry, United Kingdom*
- 57 *STFC Rutherford Appleton Laboratory, Didcot, United Kingdom*
- 58 *School of Physics and Astronomy, University of Edinburgh, Edinburgh, United Kingdom*
- 59 *School of Physics and Astronomy, University of Glasgow, Glasgow, United Kingdom*
- 60 *Oliver Lodge Laboratory, University of Liverpool, Liverpool, United Kingdom*
- 61 *Imperial College London, London, United Kingdom*
- 62 *Department of Physics and Astronomy, University of Manchester, Manchester, United Kingdom*
- 63 *Department of Physics, University of Oxford, Oxford, United Kingdom*
- 64 *Massachusetts Institute of Technology, Cambridge, MA, United States*
- 65 *University of Cincinnati, Cincinnati, OH, United States*
- 66 *University of Maryland, College Park, MD, United States*
- 67 *Los Alamos National Laboratory (LANL), Los Alamos, United States*
- 68 *Syracuse University, Syracuse, NY, United States*
- 69 *School of Physics and Astronomy, Monash University, Melbourne, Australia, associated to* ⁵⁶

- ⁷⁰ Pontifícia Universidade Católica do Rio de Janeiro (PUC-Rio), Rio de Janeiro, Brazil, associated to ²
- ⁷¹ Physics and Micro Electronic College, Hunan University, Changsha City, China, associated to ⁷
- ⁷² Guangdong Provincial Key Laboratory of Nuclear Science, Guangdong-Hong Kong Joint Laboratory of Quantum Matter, Institute of Quantum Matter, South China Normal University, Guangzhou, China, associated to ³
- ⁷³ School of Physics and Technology, Wuhan University, Wuhan, China, associated to ³
- ⁷⁴ Departamento de Física, Universidad Nacional de Colombia, Bogota, Colombia, associated to ¹³
- ⁷⁵ Universität Bonn — Helmholtz-Institut für Strahlen und Kernphysik, Bonn, Germany, associated to ¹⁷
- ⁷⁶ Institut für Physik, Universität Rostock, Rostock, Germany, associated to ¹⁷
- ⁷⁷ Eotvos Lorand University, Budapest, Hungary, associated to ⁴⁸
- ⁷⁸ INFN Sezione di Perugia, Perugia, Italy, associated to ²¹
- ⁷⁹ Van Swinderen Institute, University of Groningen, Groningen, Netherlands, associated to ³²
- ⁸⁰ Universiteit Maastricht, Maastricht, Netherlands, associated to ³²
- ⁸¹ National Research Centre Kurchatov Institute, Moscow, Russia, associated to ⁴¹
- ⁸² National Research University Higher School of Economics, Moscow, Russia, associated to ⁴²
- ⁸³ National University of Science and Technology “MISIS”, Moscow, Russia, associated to ⁴¹
- ⁸⁴ National Research Tomsk Polytechnic University, Tomsk, Russia, associated to ⁴¹
- ⁸⁵ DS4DS, La Salle, Universitat Ramon Llull, Barcelona, Spain, associated to ⁴⁵
- ⁸⁶ Department of Physics and Astronomy, Uppsala University, Uppsala, Sweden, associated to ⁵⁹
- ⁸⁷ University of Michigan, Ann Arbor, United States, associated to ⁶⁸
- ^a Universidade Federal do Triângulo Mineiro (UFMT), Uberaba-MG, Brazil
- ^b Hangzhou Institute for Advanced Study, UCAS, Hangzhou, China
- ^c Università di Bari, Bari, Italy
- ^d Università di Bologna, Bologna, Italy
- ^e Università di Cagliari, Cagliari, Italy
- ^f Università di Ferrara, Ferrara, Italy
- ^g Università di Firenze, Firenze, Italy
- ^h Università di Genova, Genova, Italy
- ⁱ Università degli Studi di Milano, Milano, Italy
- ^j Università di Milano Bicocca, Milano, Italy
- ^k Università di Modena e Reggio Emilia, Modena, Italy
- ^l Università di Padova, Padova, Italy
- ^m Scuola Normale Superiore, Pisa, Italy
- ⁿ Università di Pisa, Pisa, Italy
- ^o Università della Basilicata, Potenza, Italy
- ^p Università di Roma Tor Vergata, Roma, Italy
- ^q Università di Siena, Siena, Italy
- ^r Università di Urbino, Urbino, Italy
- ^s MSU — Iligan Institute of Technology (MSU-IIT), Iligan, Philippines
- ^t P.N. Lebedev Physical Institute, Russian Academy of Science (LPI RAS), Moscow, Russia
- ^u Novosibirsk State University, Novosibirsk, Russia
- † Deceased